AD-A075 830 NEW YORK UNIV N Y DEPT OF PHYSICS F/G 7/4
THEORY OF SATURATION SPECTROSCOPY INCLUDING COLLISIONAL EFFECTS--ETC(U)
SEP 79 P R BERMAN , P F LIAO , J E BJORKHOLM N00014-77-C-0553

UNCLASSIFIED NL

1 OF 1

AD A075830

END
DATE FILMED
11-79
DDC

Submitted to Phys. Rev. A

LEVEL II

12

AD A075830

DDC FILE COPY

6

Theory of saturation spectroscopy including collisional effects

10 P. R./Berman, P. F. /Liao J. E. /Bjorkholm

Physics Department, New York University, 4 Washington Place

New York, New York 10003

and

P. F. Liao and J. E. Bjorkholm

Bell Telephone Laboratories

Holmdel, New Jersey 07733

11 Sep 79

12 29

Supported by the U.S. Office of Naval Research under Contract No. N00014-77-C-0553.

15

Sept. 79

406 850

JOB

Abstract

A theory of saturation spectroscopy in three-level gas vapor systems, including collisional effects, is presented. Using a model of collisions in which they are phase-interrupting in their effect on level coherences and velocity-changing in their effect on level population densities, we calculate the absorption profile of a weak probe field on a given transition when an arbitrarily strong pump field acts on a coupled transition.

Line shapes are derived for an arbitrary collision kernel describing the velocity-changing collisions, and these line shapes are evaluated for the collision kernel proposed by Keilson and Storer. Various limiting forms for the line shapes are derived and representative line shapes are displayed. Several new features of the line shapes, including collisionally-induced increased probe absorption are discussed. The line shapes are seen to reflect the various collisional processes that may occur in atomic or molecular systems.

I. Introduction

The theory of saturation spectroscopy of gas vapors has received considerable attention[1-8] over the past several years, following the increased experimental activity in this field. In a typical experimental situation one uses a pump laser field to excite a given transition in an atom or molecule and then monitors the absorption of a co- or counter-propagating weak probe field on the same or a coupled transition. In general, only atoms having a limited range of longitudinal velocities can effectively interact with both the pump and the probe fields, leading to a saturation spectroscopy line shape that is essentially free of any Doppler width. The Doppler-free line widths are of the order of the natural widths associated with atomic resonances.

Saturation spectroscopy has also proven useful for collisional studies, although this area of research is only beginning to experience significant growth. Pressure broadening and shift coefficients can be precisely determined in saturation spectroscopy experiments and these parameters are related to the total collision cross sections for the states involved in the transitions. Moreover, information on differential scattering cross sections may be obtained in saturation spectroscopy using a pump laser to selectively excite atoms having a specific longitudinal velocity and a second laser to probe this velocity distribution. Since collisions modify the velocity distribution, the probe absorption serves to monitor velocity-changing collision effects. In this manner, one

obtains the differential scattering cross section averaged over perturber velocities and those transverse velocities of the active atoms not selected by the pump laser.

To fully explore the potential of saturation spectroscopy for collisional studies, it is useful to have a theory of the saturation spectroscopy line shape including collisional effects. Several theories exist[6, 9-16], but they have tended to be limited in one way or another. Some calculations are restricted to the weak pump field limit, some to the limit of decay widths and atom-field detunings much less than the Doppler width, some to the neglect of velocity-changing collisions, and some to extreme models for velocity-changing collisions. In this paper, we present a calculation of the saturation spectroscopy line shape in a three-level atomic system including collisional effects. A pump field of arbitrary strength drives a given transition and the absorption spectrum of a weak probe field on a coupled transition is derived. The calculation is based on a simple but often applicable collision model in which collisions are phase-interrupting in their effect on level coherences (off-diagonal density matrix elements) and velocity-changing in their effect on level populations. The only restrictions on level widths, collision rates, and detunings are those implied by the impact approximation.[11]

In Secs. II and III, general equations are derived for the probe field absorption, and a specific calculation is carried out using the

Keilson-Storer collision kernel in a large-angle scattering limit. Limiting forms of the line shape for weak-pump fields, for large pump-field detunings, and for decay rates and detunings less than the Doppler width (Doppler limit) are given in Sec. IV and some representative line shapes displayed in Sec. V. An appendix generalizes the results to allow for an inelastic decay channel for the intermediate state.

The line shapes illustrated in Sec. V contain some features that are either new or have not been emphasized in the past. Among these are (1) a relatively large dispersion-like contribution to the line shape that appears for pump-field detunings greater than the Doppler width, (2) ac Stark splittings of the profiles in strong pump fields for <u>both</u> co- and counter-propagating fields, and (3) modifications of the strong-pump-field line profiles produced by velocity-changing collisions. An additional feature of the strong-pump-field line shapes discussed in Sec. V is a collision-induced <u>increase</u> in both the maximum and integrated probe-field absorption. This result has implications for increasing yields in certain laser isotope separation schemes.

By necessity, this paper contains a large number of equations. The reader not interested in the details of the calculation can obtain the physical ideas by making reference to Secs. II. A - B and proceeding directly to Sec. V. The theory has recently been used to explain the $3S_{1/2} - 3P_{1/2} - 4D_{3/2}$ excitation line shapes of Na in the presence of foreign gas perturbers.[17]

II. Physical System - Equations of Motion

A. Physical System Neglecting Collisions

The three-level atomic systems to be considered are shown in Fig. 1. The quantities $\beta = \pm 1$, $\beta' = \pm 1$ label each of the level configurations so that they may all be treated by a single formalism. For the upward cascade (Fig. 1a), $\beta = \beta' = 1$; for the inverted V (Fig. 1b), $\beta = 1$, $\beta' = -1$; and for the V configuration (Fig. 1c) $\beta = -1$, $\beta' = 1$. Each of the levels i is incoherently pumped with a rate density $\lambda_i(\vec{v})$ and each level decays at some rate γ_i, owing to spontaneous emission. The $\lambda_i(\vec{v})$ are assumed to produce equilibrium distributions in the absence of any fields - i.e. collisions do not alter the $\lambda_i(\vec{v})$. Levels 1 and 3 are assumed to have the same parity which is opposite to that of level 2. The 1-2 and 2-3 transition frequencies are denoted by ω and ω', respectively. Note that it is possible to allow for any of the lowest lying levels to be a ground state by taking the limit $\lambda(\vec{v})\to 0$, $\gamma\to 0$, $\lambda(\vec{v})/\gamma \to N_o(\vec{v})$ (finite) for that level.

To include some effects of branching that occur in real physical systems, spontaneous emission from level 2 to level 1 at some rate γ_2' is included in the model (of course, $\gamma_2' = 0$ for the V configuration of Fig. 1c). Extensions of the theory to allow for additional spontaneous emission branching channels between the levels is straightforward.

The three-level systems are subjected to an arbitrarily strong monochromatic pump field

$$\vec{\mathcal{E}}(\vec{R},t) = \hat{\imath}\,\mathcal{E}\cos(kZ-\Omega t) \tag{1a}$$

and a weak monochromatic probe field

$$\vec{\mathcal{E}}'(\vec{R},t) = \hat{\imath}\,\mathcal{E}'\cos(\epsilon k' Z-\Omega' t), \tag{1b}$$

the fields having frequencies Ω, Ω' and propagation vectors

$$\vec{k} = \hat{z}\,\Omega/c \quad ; \quad \vec{k}' = \hat{z}\,\Omega'/c \tag{2}$$

respectively. Our discussion is limited to the case of copropagating ($\epsilon = 1$) or counterpropagating ($\epsilon = -1$) laser fields. It is assumed that fields E and E' are nearly resonant with the 1-2 and 2-3 transitions, respectively. Furthermore, it is assumed that the difference $|\omega-\omega'|$ is large enough to insure that field $\vec{E}$ drives only the 1-2 transition and $\vec{E}'$ only the 2-3 transition.

The calculation is most conveniently performed using equations for density matrix elements. In the absence of collisions, the master equation for density matrix elements $\rho_{ij}(\vec{R},\vec{v},t)$ associated with an atomic wave packet centered at $\vec{R}$ moving with average velocity $\vec{v}$ at time t is[18]

$$\begin{aligned}\partial\rho_{ij}(\vec{R},\vec{v},t)/\partial t &+ \vec{v}\cdot\vec{\nabla}\rho_{ij}(\vec{R},\vec{v},t)\\ &= (i\hbar)^{-1}\left[H(\vec{R},t),\rho(\vec{R},\vec{v},t)\right]_{ij} - \gamma_{ij}\rho_{ij}(\vec{R},\vec{v},t)\\ &\quad + \gamma_2'\,\delta_{i1}\delta_{j1}\,\rho_{22}(\vec{R},\vec{v},t) + \lambda_i(\vec{v})\,\delta_{ij} \quad ;\end{aligned} \tag{3}$$

where

$$\gamma_{ij} = \frac{1}{2}(\gamma_i + \gamma_j). \tag{4}$$

Matrix elements of the Hamiltonian H are given by

$$H_{ij}(\vec{R},t) = E_i \delta_{ij} - p_{ij}\left[\mathcal{E}(\vec{R},t) + \mathcal{E}'(\vec{R},t)\right] \tag{5}$$

where E_i is the energy of level i and p_{ij} is the x component of the dipole matrix element between states i and j.

B. Collision Model

The three-level active atoms undergo collisions with ground-state perturbers. The following assumptions, pertaining to the nature of the collisions and the duration τ_c of a collision, are incorporated into the model: (1) the active-atom and perturber densities are such that one can neglect all but binary active atom-perturber collisions. (2) Resonant excitation-exchange collisions between active atoms and perturbers are excluded. (3) Collisions are adiabatic in the sense that they can not, in the absence of applied fields, induce transitions between levels 1, 2 and 3 shown in Fig. 1 (i.e. $\hbar\tau_c^{-1}$ << all level spacings). (4) Collisions may be treated in the impact approximation, in which collisions can be thought to occur instantaneously with respect to various time scales in the problem (valid if τ_c^{-1} >> atom-field detunings, Rabi frequencies, collision and decay rates).

With these approximations, the net effect of collisions is the addition of a term $\partial\rho_{ij}(\vec{R},\vec{v},t)/\partial t)_{coll}$ to the r.h.s. of Eq. (3).[18]

In general collisions affect off-diagonal and diagonal density matrix elements differently. For diagonal elements, collisions result solely in velocity-changes and the collisional evolution of the population densities is governed by the usual transport equation

$$\partial\rho_{ii}(\vec{R},\vec{v},t)/\partial t)_{coll} = -\Gamma_i(\vec{v})\,\rho_{ii}(\vec{R},\vec{v},t) + \int d\vec{v}'\,W_i(\vec{v}'\to\vec{v})\,\rho_{ii}(\vec{R},\vec{v}',t) \tag{6}$$

where, $W_i(\vec{v}'\to\vec{v})$ is the kernel and

$$\Gamma_i(\vec{v}) = \int d\vec{v}'\,W_i(\vec{v}\to\vec{v}') \tag{7}$$

the rate for collisions in level i. One can use either classical or quantum-mechanical expressions[12] for the kernels and rates. The kernel is simply the differential scattering cross section in the center-of-mass system, averaged over the perturber velocity distribution consistent with energy and momentum conservation.

Collisional effects on off-diagonal density matrix elements are more complex. We adopt a model in which collisions are "phase-interrupting" in their effect on off-diagonal density matrix elements, leading to a time rate of change

$$\partial\rho_{ij}(\vec{R},\vec{v},t)/\partial t)_{coll} = -\left[\Gamma_{ij}^{ph}(\vec{v}) + i S_{ij}^{ph}(\vec{v})\right]\rho_{ij}(\vec{R},\vec{v},t) \qquad i \neq j \tag{8}$$

where $\Gamma_{ij}^{ph}(\vec{v})$ and $S_{ij}^{pj}(\vec{v})$ are broadening and shift parameters common to theories of pressure broadening.[9,16] The phase-interruption model is valid for either (a) a low perturber to active-atom mass ratio or (b) strongly

state-dependent collisional interactions.[12]

In subsection D, a final assumption, limiting the calculation to large angle scattering is made. The reader not interested in the details of the line shape calculation can proceed to Sec. III without loss of continuity.

C. Steady-State Equations

Adding Eqs. (6) or (8) to (3), introducing the field interaction representation

$$\rho_{12}(\vec{R},\vec{v},t) = \tilde{\rho}_{12}(\vec{v},t)\ \exp[-i\beta(kZ-\Omega t)] \tag{9a}$$

$$\rho_{23}(\vec{R},\vec{v},t) = \tilde{\rho}_{23}(\vec{v},t)\ \exp[-i\beta'(\epsilon k'Z-\Omega' t)] \tag{9b}$$

$$\rho_{13}(\vec{R},\vec{v},t) = \tilde{\rho}_{13}(\vec{v},t)\ \exp\{-i[(\beta k+\epsilon\beta' k')Z-(\beta\Omega+\beta'\Omega')t]\} \tag{9c}$$

$$\tilde{\rho}_{ij}(\vec{v},t) = \tilde{\rho}_{ji}(\vec{v},t)^{*} \tag{9d}$$

$$\rho_{ii}(\vec{R},\vec{v},t) = \tilde{\rho}_{ii}(\vec{v},t) \tag{9e}$$

making the rotating-wave approximation and setting $\partial\tilde{\rho}_{ij}(\vec{v},t)/\partial t = 0$, one obtains the following steady-state equations:

$$\Gamma_1^t(\vec{v})\,\tilde{\rho}_{11}(\vec{v}) = \int d\vec{v}'\, W_1(\vec{v}'\to\vec{v})\,\tilde{\rho}_{11}(\vec{v}') + i\chi[\tilde{\rho}_{21}(\vec{v})-\tilde{\rho}_{12}(\vec{v})] + \lambda_1(\vec{v}) + \gamma_2'\tilde{\rho}_{22}(\vec{v}) \tag{10a}$$

$$\Gamma_2^t(\vec{v})\,\tilde{\rho}_{22}(\vec{v}) = \int d\vec{v}'\, W_2(\vec{v}'\to\vec{v})\,\tilde{\rho}_{22}(\vec{v}') - i\chi[\tilde{\rho}_{21}(\vec{v})-\tilde{\rho}_{12}(\vec{v})] - i\chi'[\tilde{\rho}_{23}(v)-\tilde{\rho}_{32}(\vec{v})] + \lambda_2(\vec{v}) \tag{10b}$$

$$\Gamma_3^t(\vec{v})\,\tilde{\rho}_{33}(\vec{v}) = \int d\vec{v}'\, W_3(\vec{v}'\to\vec{v})\,\tilde{\rho}_{33}(\vec{v}') + i\chi'[\tilde{\rho}_{23}(\vec{v})-\tilde{\rho}_{32}(\vec{v})] + \lambda_3(\vec{v}) \tag{10c}$$

$$\mu_{12}(\vec{v})\tilde{\rho}_{12}(\vec{v}) = i\chi[\tilde{\rho}_{22}(\vec{v})-\tilde{\rho}_{11}(\vec{v})] - i\chi'\tilde{\rho}_{13}(\vec{v}) \tag{10d}$$

$$\mu_{23}(\vec{v})\tilde{\rho}_{23}(\vec{v}) = i\chi'[\tilde{\rho}_{33}(\vec{v})-\tilde{\rho}_{22}(\vec{v})] + i\chi\tilde{\rho}_{13}(\vec{v}) \tag{10e}$$

$$\mu_{13}(\vec{v})\tilde{\rho}_{13}(\vec{v}) = i\chi\tilde{\rho}_{23}(\vec{v}) - i\chi'\tilde{\rho}_{12}(\vec{v}) \tag{10f}$$

$$\tilde{\rho}_{ij}(\vec{v}) = \tilde{\rho}_{ji}(\vec{v})^{*} \tag{10g}$$

where

$$\mu_{12}(\vec{v}) = [\gamma_{12} + \Gamma_{12}^{ph}(\vec{v})] + i[\beta(\Delta - kv_z) + S_{12}^{ph}(\vec{v})] \tag{11a}$$

$$\mu_{23}(\vec{v}) = [\gamma_{23} + \Gamma_{23}^{ph}(\vec{v})] + i[\beta'(\Delta' - \epsilon k'v_z) + S_{23}^{ph}(\vec{v})] \tag{11b}$$

$$\mu_{13}(\vec{v}) = [\gamma_{13} + \Gamma_{13}^{ph}(\vec{v})] + i[(\beta\Delta+\beta'\Delta') - (\beta k+\beta'\epsilon k')v_z + S_{13}^{ph}(\vec{v})] \tag{11c}$$

$$\Gamma_i^t(\vec{v}) = \gamma_i + \Gamma_i(\vec{v}) \tag{12}$$

$$\chi = p_{12}\mathcal{E}/2\hbar \quad ; \quad \chi' = p_{23}\mathcal{E}'/2\hbar \tag{13}$$

with the detunings Δ and Δ' defined as

$$\Delta = \Omega - \omega \quad ; \quad \Delta' = \Omega' - \omega' \tag{14}$$

The normalization is such that $\int \rho_{ii}(\vec{v})\, d\vec{v}$ represents the total ensemble population in level i.

Typically one measures the probe field absorption, which is equivalent to determining the value of

$$I(\Delta,\Delta') = \int d\vec{v}\,[\tilde{\rho}_{33}(\vec{v}) - \lambda_3(\vec{v})/\gamma_3] \tag{15}$$

Using Eqs. (10c), (12) and (7), this equation can be rewritten as

$$I(\Delta,\Delta') = -2(\chi'/\gamma_3)\,\mathrm{Im}\int d\vec{v}\,\tilde{\rho}_{23}(\vec{v}) \tag{16}$$

It is sufficient to calculate $\tilde{\rho}_{23}(\vec{v})$ to determine the line shape.

The solution of Eqs. (10) for $\tilde{\rho}_{23}(\vec{v})$ to first order in χ' (weak probe field) and arbitrary order in χ (weak or strong pump field) is[1-7]

$$\tilde{\rho}_{23}(\vec{v}) = \frac{-i\chi'}{\mu_{13}(\vec{v})\mu_{23}(\vec{v})+\chi^2}\left\{\mu_{13}(\vec{v})[\tilde{\rho}^{(0)}_{22}(\vec{v})-\tilde{\rho}^{(0)}_{33}(\vec{v})]+i\chi\tilde{\rho}^{(0)}_{12}(\vec{v})\right\} \tag{17}$$

where the $\tilde{\rho}^{(0)}_{ij}(\vec{v})$ are solutions to Eqs. (10) with $\chi' = 0$.

It is convenient to rearrange the equations for $\tilde{\rho}^{(0)}_{ij}(\vec{v})$ in order to isolate some of the strong field effects. First, we write each $\tilde{\rho}^{(0)}_{ii}(\vec{v})$ as a sum of its value $N_i(\vec{v})$ in the absence of fields plus a remainder $n_i(\vec{v})$. Explicitly

$$\tilde{\rho}^{(0)}_{ii}(\vec{v}) = N_i(\vec{v}) + n_i(\vec{v}) \tag{18}$$

where

$$\begin{aligned} N_1(\vec{v}) &= \lambda_1(\vec{v})/\gamma_1 + \gamma_2'\lambda_2(\vec{v})/\gamma_1\gamma_2 \\ N_2(\vec{v}) &= \lambda_2(\vec{v})/\gamma_2 \\ N_3(\vec{v}) &= \lambda_3(\vec{v})/\gamma_3 \end{aligned} \tag{19}$$

Second, we substitute Eqs. (19) into Eqs. (10), set $\chi' = 0$, use the fact that

$$\int d\vec{v}'\,W_i(\vec{v}'\to\vec{v})\,N_i(\vec{v}') = \Gamma_i(\vec{v})\,N_i(\vec{v}) \tag{20}$$

(since the $N_i(\vec{v})$ are assumed to be equilibrium distributions), and perform some algebraic manipulations of the resulting equations. Using this procedure, we obtain the following equations for $n_i(\vec{v})$ and $\rho^{(0)}_{ij}(\vec{v})$ $(i \neq j)$:

$$\begin{aligned} \Gamma_1^{e}(\vec{v})n_1(\vec{v}) - \int d\vec{v}'\,W_1(\vec{v}'\to\vec{v})n_1(\vec{v}') &= [2\chi^2\tilde{\gamma}_{12}(\vec{v})/R_B(\vec{v})^2][1-\gamma_2'/\Gamma_2^{e}(\vec{v})][N_{21}(\vec{v})+\tilde{F}(\vec{v})] \\ &\quad +[\gamma_2'/\Gamma_2^{e}(\vec{v})]\int d\vec{v}'\,W_2(\vec{v}'\to\vec{v})n_2(\vec{v}') \end{aligned} \tag{21a}$$

$$\Gamma_2^{e}(\vec{v})n_2(\vec{v}) - \int d\vec{v}'\,W_2(\vec{v}'\to\vec{v})n_2(\vec{v}') = -[2\chi^2\tilde{\gamma}_{12}(\vec{v})/R_B(\vec{v})^2][N_{21}(\vec{v})+\tilde{F}(\vec{v})] \tag{21b}$$

$$\tilde{\rho}^{(0)}_{12}(\vec{v}) = [i\chi\mu_{12}(\vec{v})^*/R_B(\vec{v})^2][N_{21}(\vec{v})+\tilde{F}(\vec{v})] \tag{21c}$$

$$n_3(\vec{v}) = \tilde{\rho}^{(0)}_{23}(\vec{v}) = \tilde{\rho}^{(0)}_{13}(\vec{v}) = 0 \tag{21d}$$

where

$$\tilde{\gamma}_{12}(\vec{v}) = \gamma_{12} + \Gamma^{ph}_{12}(\vec{v}) \tag{22}$$

$$R_B(\vec{v})^2 = \gamma_B(\vec{v})^2 + [\Delta - kv_z + \beta S^{ph}_{12}(\vec{v})]^2 \tag{23}$$

$$\gamma_B(\vec{v}) = \tilde{\gamma}_{12}(\vec{v})[1+\mathcal{J}(\vec{v})]^{1/2} \tag{24}$$

$$\mathcal{S}(\vec{v}) = \frac{2\chi^2}{\tilde{\gamma}_{12}(\vec{v})}\left[\frac{1}{\Gamma_2^t(\vec{v})} + \frac{1}{\Gamma_1^t(\vec{v})}\left(1 - \frac{\gamma_2'}{\Gamma_2^t(\vec{v})}\right)\right] \tag{25}$$

$$\tilde{\sigma}(\vec{v}) = \frac{1}{\Gamma_2^t(\vec{v})}\left(1 - \frac{\gamma_2'}{\Gamma_1^t(\vec{v})}\right)\int d\vec{v}'\, W_2(\vec{v}' \to \vec{v})\, n_2(\vec{v}') - \frac{1}{\Gamma_1^t(\vec{v})}\int d\vec{v}'\, W_1(\vec{v}' \to \vec{v})\, n_1(\vec{v}') \tag{26}$$

$$N_{ij}(\vec{v}) = N_i(\vec{v}) - N_j(\vec{v}) \tag{27}$$

Moreover, Eq. (17) may be written

$$\tilde{\rho}_{23}(\vec{v}) = \frac{-i\chi'}{\mu_{13}(\vec{v})\mu_{23}(\vec{v}) + \chi^2}\left\{\mu_{13}(\vec{v})[-N_{32}(\vec{v}) + n_2(\vec{v})] + i\chi\tilde{\rho}_{12}^{(0)}(\vec{v})\right\} \tag{28}$$

The line shape, as determined by Eqs. (16) and (21-28), contains some features that may be noted at this point:

(i) Velocity-changing collisions in level 3 do not affect the line shape, a result which may be explained by the following reasoning. The probe field is weak, so that one need consider only a single probe field absorption process. If velocity-changing collisions in level 3 occur <u>before</u> the probe field absorption, they do not alter the equilibrium distribution $N_3(\vec{v})$. If they occur <u>after</u> the probe field absorption,

they redistribute the velocities in level 3, but do not change the integrated population $\int \rho_{33}(\vec{v})\, d\vec{v}$, on which the line shape is dependent.

(ii) In the absence of collisions $[F \to 0,\ W_i(\vec{v}' \to \vec{v}) \to 0,\ \Gamma_{ij}^{ph}(\vec{v}) \to 0,\ S_{ij}^{ph}(\vec{v}) \to 0,\ \Gamma_i^t(\vec{v}) \to \gamma_i]$, Eqs. (21) reduce to well-known equations of saturation spectroscopy.[1-8] The strong field modification of the 1-2 absorption is contained in Eqs. (23-25), in which the homogeneous width γ_{12} is replaced by a power broadened γ_B. The factor $\chi^2\tilde{\gamma}_{12}(\vec{v})N_{21}(\vec{v})[R_B(\vec{v})]^{-2}$ appearing in Eqs. (21) represents holes or bumps created in the velocity distribution by the pump field.

(iii) One can understand the collision-induced modification of the 1-2 strong-field absorption on the basis of simple physical arguments. Phase-changing collisions are directly incorporated with the substitution $\gamma_{12} \to \tilde{\gamma}_{12}(\vec{v})$, $\Delta_{12} \to \delta\Delta + S_{12}^{ph}(\vec{v})$, representing the traditional pressure broadening and shifting of spectral profiles. Velocity-changing collisions in levels 1 and 2 lead to flow into and out of the velocity holes created in these population densities by the pump field. New velocity equilibrium distributions are established, as given by the solutions of Eqs. (21a-b). The outward flow is contained in the $\Gamma_i^t(v)\, n_i(\vec{v})$ terms in Eqs. (21a-b); it is also implicitly contained in the saturation parameter $S(\vec{v})$ through the presence of $\Gamma_i^t(\vec{v})$. The inward flow is given by the $\int d\vec{v}'\, W_i(\vec{v}' \to \vec{v})\, n_i(\vec{v}')$ terms and the $F(\vec{v})$ terms in Eqs. (21a-c).

D. Large-Angle Scattering

Equations (21) are independent of the specific nature of the scattering (velocity-changing collisions) in levels 1 and 2

and could, in principle, be solved numerically for an arbitrary kernel. However, it is customary to seek approximate solutions to the equations. For weak velocity-changing collisions, $k\Delta u \lesssim \gamma_B$, ($\Delta u$ = rms velocity change per collision), one can approximate the collision kernels as functions of $(\vec{v}-\vec{v}')$ and obtain solutions by Fourier transform techniques.[13,14,19] Exact solutions are also obtainable[20] in the so called "strong collision model" in which a single collision, on average, thermalizes the velocity distribution.

For typical interatomic potentials, the collision kernels can be separated into a small-angle scattering part accounting for the long-range part of the potential plus a large angle scattering (LAS) part accounting for scattering from deep attractive potential wells and/or a repulsive core. As a specific model, we will consider only the LAS part of the kernel, assuming weak collisional effects are negligible or can otherwise be incorporated into the line shape formulas.

The kernel is defined to be a LAS one provided

$$k\Delta u > \gamma_B \tag{29}$$

In this limit, a single collision is sufficient to remove atoms from the velocity holes or bumps created by the fields. There is no velocity diffusion <u>within</u> a hole or bump. The F terms in Eqs. (21a-c) represent the modifications of the bumps or holes owing to velocity-changing collisions; consequently, they should vanish in this model. An estimate of the value of $F(\vec{v})$ relative to $N_{21}(\vec{v})$ at $\vec{v} = (\Delta/k)\hat{z}$ is

$$\tilde{F}/N_{21} \lesssim \pi^{1/2}\gamma_B/(k\Delta u) \tag{30}$$

which will be small provided $\gamma_B/k\Delta u \ll 1$. Calculations using a more general collision model[19] indicate that the LAS kernel provides a good approximation as long as $\gamma_B/k\Delta u < 1$.

Thus, in the LAS model, the equations determining $n_2(\vec{v})$ and $\tilde{\rho}_{12}^{(0)}(\vec{v})$ needed in Eq. (28) are

$$\Gamma_2^t(\vec{v})\, n_2(\vec{v}) - \int d\vec{v}'\, W_2(\vec{v}'\to\vec{v})\, n_2(\vec{v}') = -\left[2\chi^2\tilde{\gamma}_{12}(\vec{v})/R_B(\vec{v})^2\right] N_{21}(\vec{v}) \tag{31a}$$

$$\tilde{\rho}_{12}^{(0)}(\vec{v}) = \left[i\chi\,\mu_{12}(\vec{v})^*/R_B(\vec{v})^2\right] N_{21}(\vec{v}) \tag{31b}$$

These equations differ from those of the weak field case only by the presence of γ_B rather than $\tilde{\gamma}_{12}(\vec{v})$ in the term for $R_B(\vec{v})$.

One final separation is useful regardless of the kernel. A solution for $n_2(\vec{v})$ can always be written in the form

$$n_2(\vec{v}) = n_2^{(0)}(\vec{v}) + \delta n_2(\vec{v}) \tag{32a}$$

where

$$n_2^{(0)}(\vec{v}) = -2\chi^2\tilde{\gamma}_{12}(\vec{v})\, N_{21}(\vec{v})/\left[R_B(\vec{v})^2\,\Gamma_2^t(\vec{v})\right] \tag{32b}$$

and $\delta n_2(\vec{v})$, representing the velocity redistribution of the holes or bumps created by the pump field, satisfies

$$\Gamma_2^t(\vec{v})\,\delta n_2(\vec{v}) - \int d\vec{v}'\, W_2(\vec{v}'\to\vec{v})\,\delta n_2(\vec{v}') = \int d\vec{v}'\, W_2(\vec{v}'\to\vec{v})\, n_2^{(0)}(\vec{v}'), \tag{32c}$$

III. Saturation Spectroscopy Line Shape

Within the confines of the collision model adopted in Sec. II.A, the probe absorption line profile is given by Eqs. (16), (28), (11), (27), (18) and (21). In saturation spectroscopy, one can arrange to detect only that part of the probe field absorption influenced by the presence of the laser pump field. More precisely, one measures the probe field absorption <u>minus</u> the probe field absorption in the absence of the laser pump (i.e. $\chi \to 0$). Denoting this quantity by $I_s(\Delta, \Delta')$, we find from Eqs. (16) and (18) that

$$I_s(\Delta, \Delta') = I(\Delta, \Delta') + \frac{2(\chi')^2}{\gamma_3} \mathrm{Re} \int d\vec{v}\, \frac{N_{32}(\vec{v})}{\mu_{23}(\vec{v})} \tag{33}$$

To arrive at our final line shape formula, three additional assumptions are made. First, the velocity or speed-dependence of $\Gamma_{ij}^{ph}(\vec{v})$, $S_{ij}^{ph}(\vec{v})$ and $\gamma_i(\vec{v})$ is neglected. Generally, this approximation is not drastic since these quantities are slowly varying functions of $\vec{v}$ that may be evaluated at some appropriate fixed value of $\vec{v}$ without introducing much error. <u>Second, it is assumed that velocity-changing collisions in level 2 are characterized by the large-angle-scattering limit (LAS) discussed in Sec. II.D.</u> Consequently $n_2(\vec{v})$ and $\tilde{\rho}_{12}^{(0)}(\vec{v})$ are determined from Eqs. (31) rather than (21). Finally, the $N_{ij}(\vec{v})$ are taken to be Maxwellian.

$$N_{ij}(\vec{v}) = N_{ij}(\pi u^2)^{-3/2} \exp(-v^2/u^2) \tag{34}$$

The saturation spectroscopy line shape is determined from Eqs. (33), (16), (28), (11), (27), (18), (31), (32) and (34). The integrals

can be evaluated[7] in terms of plasma dispersion functions and the result is conveniently separated into four terms as follows:

$$I_s(\Delta, \Delta') = I_{12}^{Ta} + I_{nvc}^{sw} + I_{vc}^{sw} + I_{23}^{Ta} \tag{35}$$

where

$$I_{12}^{Ta} = \frac{-2(\chi\chi')^2 N_{21}\, \theta_{12}\, \theta_{23}\, \theta_{13}}{\gamma_3\, ku\, k'u\, k''u}\, \mathrm{Im} \sum_{j=1}^{4} A_j \tilde{Z}(r_j) \tag{36a}$$

$$I_{nvc}^{sw} = \frac{4(\chi\chi')^2 N_{21}\, \tilde{\gamma}_{12}\, \theta_{23}}{\gamma_3\, \Gamma_2^t (ku)^2\, k'u}\, \mathrm{Im} \sum_{j=1}^{4} D_j \tilde{Z}(r_j) \tag{36b}$$

$$I_{vc}^{sw} = \frac{2(\chi')^2}{\gamma_3}\, \mathrm{Re} \int d\vec{v}\, \frac{\mu_{13}(\vec{v})\, \delta n_2(\vec{v})}{\mu_{12}(\vec{v})\, \mu_{23}(\vec{v}) + \chi^2} \tag{36c}$$

$$I_{23}^{Ta} = \frac{2(\chi')^2 N_{32}\, \theta_{23}}{\gamma_3\, k'u}\, \mathrm{Im}\Big[\sum_{j=1}^{2} B_j \tilde{Z}(r_j) - \tilde{Z}(r_7)\Big] \tag{36d}$$

$$r_1 = r_6 + C \tag{37a}$$

$$r_2 = r_7 - C \tag{37b}$$

$$r_3 = i\eta_0^- / (k_{12}u) \tag{37c}$$

$$r_4 = -i\eta_8 / (k_{12}u) = r_3^* \tag{37d}$$

$$r_5 = i\eta_{12}^* / (k_{12}u) \tag{37e}$$

$$r_6 = -i\eta_{13} / (k_{13}u) \tag{37f}$$

$$r_7 = -i\eta_{23} / (k_{23}u) \tag{37g}$$

$$C = \frac{1}{2}\left\{ r_7 - r_6 - \left[(r_7 - r_6)^2 + \frac{4x^2}{k_{13}u\, k_{23}u} \right]^{1/2} \right\} \tag{37h}$$

$$\eta_{12} = \tilde{\gamma}_{12} + i\,\Delta_{12} \tag{38a}$$

$$\eta_{23} = \tilde{\gamma}_{23} + i\,\Delta_{23} \tag{38b}$$

$$\eta_{13} = \tilde{\gamma}_{13} + i\,\Delta_{13} \tag{38c}$$

$$\eta_B = \gamma_B + i\,\Delta_{12} \tag{38d}$$

$$\Delta_{12} = \beta\Delta + S_{12}^{ph} \tag{39a}$$

$$\Delta_{23} = \beta'\Delta' + S_{23}^{ph} \tag{39b}$$

$$\Delta_{13} = \beta\Delta + \beta'\Delta' + S_{13}^{ph} \tag{39c}$$

$$\tilde{\gamma}_{ij} = \gamma_{ij} + \Gamma_{ij}^{ph} \tag{40a}$$

$$\gamma_B = \gamma_{12}\,(1 + \mathcal{S})^{1/2} \tag{40b}$$

$$\mathcal{S} = \frac{2x^2}{\tilde{\gamma}_{12}}\left[\frac{1}{\Gamma_2^t} + \frac{1}{\Gamma_1^t}\left(1 - \frac{\gamma_2'}{\Gamma_2^t}\right)\right] \tag{40c}$$

$$\Gamma_i^t = \gamma_i + \Gamma_i \tag{40d}$$

$$x = p_{12}\,\mathcal{E}/2\hbar \;;\quad x' = p_{23}\,\mathcal{E}/2\hbar \tag{41}$$

$$k_{12} = \rho k \equiv \theta_{12} k \;;\quad \theta_{12} = \rho \tag{42a}$$

$$k_{23} = \epsilon\rho' k \equiv \theta_{23} k' \;;\quad \theta_{23} = \epsilon\rho' \tag{42b}$$

$$k_{13} = \rho k + \epsilon\rho' k' \equiv \theta_{13} k'' \;;\quad k'' = |k_{13}| \;;\quad \theta_{13} = k_{13}/k'' \tag{42c}$$

$$A_i = (r_5 - r_i)\left[\prod_{j=1,4;\, j\neq i} (r_j - r_i)\right]^{-1} \tag{43a}$$

$$B_1 = (r_6 - r_1)/(r_2 - r_1) \;;\quad B_2 = (r_6 - r_2)/(r_1 - r_2) \tag{43b}$$

$$D_i = (r_6 - r_i)\left[\prod_{j=1,4;\, j\neq i} (r_j - r_i)\right]^{-1} \tag{43c}$$

subject to

$$\sum_{j=1}^{4} A_j = \sum_{j=1}^{4} D_j = 0 \;;\quad B_1 + B_2 = 1 \tag{44}$$

N_{ij} = population difference between levels i and j in the absence of external fields (45)

$$\tilde{Z}(r) = \begin{cases} Z(r) & \text{for } r > 0 \\ -Z(-r) & \text{for } r < 0 \end{cases} \tag{46}$$

where $Z(r)$ is the plasma dispersion function

$$Z(r) = -\pi^{-1/2}\int_{-\infty}^{\infty} dx\; e^{-x^2}(r \pm x)^{-1} \tag{47}$$

defined for $\mathrm{Im}(r) > 0$.

The terms appearing in Eq.(35) are designated as follows: (1) I_{12}^{TQ} is a two-quantum contribution to the line shape proportional to the inversion N_{21} (the label "two-quantum" is used to specify that such contributions vanish unless pump and probe fields are simultaneously present), (2) I_{nvc}^{SW} is a contribution resulting from the "stepwise" absorption of pump and probe photons by atoms that have not undergone velocity-changing collisions in level 2, (3) I_{vc}^{SW} is the corresponding contribution from atoms that have undergone velocity-changing collisions in level 2; this term reflects the way in which the velocity holes or bumps in level 2 created by the pump field are redistributed by collisions, (4) I_{23}^{TQ} is a two-quantum contribution to the line shape proportional to N_{32}. The labeling and interpretation of each of these terms has been given elsewhere.[11]

Equations (36a, b, d) are easily evaluated using an efficient program for the Plasma Dispersion Function.[21] However, one must specify a collision kernel, $W_2(\vec{v}'\to\vec{v})$ before Eq. (36c) can be calculated.

Independent of kernel, Eq. (36c) can be put in a more transparent form. It follows from Eqs. (32) that a propagator $\delta G_2(\vec{v}'\to\vec{v})$, defined by

$$\delta n_2(\vec{v}) = \int d\vec{v}'\, \delta G_2(\vec{v}'\to\vec{v})\, n_2^{(0)}(\vec{v}') \tag{48}$$

satisfies the equation

$$\Gamma_2^t\, \delta G_2(\vec{v}'\to\vec{v}) - \int d\vec{v}''\, W_2(\vec{v}''\to\vec{v})\, \delta G_2(\vec{v}'\to\vec{v}'') = W_2(\vec{v}'\to\vec{v}) \tag{49}$$

Using Eqs. (36c), (11), (48), (32b), (23) and (37), one can rewrite I_{vc}^{SW} in the form

$$I_{vc}^{SW} = \frac{4(\chi\chi')^2\, \tilde{\gamma}_{12}\, \theta_{23}\, u^6}{\gamma_3 (ku)^2\, k'u\, \Gamma_2^t}\, \mathrm{Im} \iint d\vec{x}\, d\vec{y}$$

$$\times \frac{(x_z - r_6)\, \delta G_2(u\vec{y}\to u\vec{x})\, N_{21}(u\vec{y})}{(x_z - r_1)(x_z - r_2)(y_z - r_3)(y_z - r_4)} \tag{50}$$

In the form (50), one can readily identify (a) the original velocity distribution $N_{21}(u\vec{y})$, (b) resonance denominators with width $\mathrm{Im}\ r_3 = \gamma_B$ representing the 1-2 absorption by atoms having velocity $u\vec{y}$, (c) the propagator $\delta G_2(u\vec{y}\to u\vec{x})$ representing the collisional redistribution of

velocities from $u\vec{y}$ to $u\vec{x}$, and (d) terms representing the probe absorption from level 2 by atoms having velocity $u\vec{x}$. To evaluate Eq. (50), one must solve Eq. (49) for $\delta G_2(\vec{v}'\to\vec{v})$. Although a formal quantum-mechanical expression for $W_2(\vec{v}'\to\vec{v})$ is available, its evaluation presents many problems. For this reason one often attempts to approximate the true kernel by an analytically tractable phenomenological one.

Keilson-Storer Kernel (KSK)

In this paper, we explicitly evaluate Eq. (50) for the collision kernel proposed by Keilson and Storer,[22]

$$W_2(\vec{v}'\to\vec{v}) = \Gamma_2(\pi\tilde{u}^2)^{-3/2}\exp\left[-(\vec{v}-\alpha\vec{v}')^2/\tilde{u}^2\right] \tag{51a}$$

$$\tilde{u}^2 = (1-\alpha^2)^{1/2}u \tag{51b}$$

where Γ_2 is the collision rate and α and $\tilde{u}$ are constants. For atoms having velocity $\vec{v}'$, the average velocity following a collision is $\alpha\vec{v}'$ (this condition restricts α to values between 0 and 1) and the one-dimensional rms spread in velocities following a collision is $\left(\frac{1}{\sqrt{2}}\right)\tilde{u} \equiv (\Delta u)$. For our LAS model, Eq. (29) further restricts α to values such that

$$(1-\alpha^2)^{1/2} > \gamma_B/ku \tag{52}$$

The Keilson-Storer Kernel (KSK) adequately describes small angle scattering.[22] Provided $v' < u$, it also describes LAS reasonably well, but is in error for both LAS and $v' \geq u$.[17] The kernel has the additional advantage that it obeys detailed balancing, and allows analytical solutions to be obtained.

If the KSK is inserted in Eq. (49) for the propagator, one can obtain the solution

$$\delta G_2(\vec{v}'\to\vec{v}) = \sum_{n=1}^{\infty}\left(\frac{\Gamma_2}{\Gamma_2^t}\right)^n \frac{1}{[\pi(\sigma_n u)^2]^{3/2}}\exp\left[-\left(\frac{\vec{v}-\alpha^n\vec{v}'}{\sigma_n u}\right)^2\right] \tag{53a}$$

$$\sigma_n = (1-\alpha^{2n})^{1/2} \tag{53b}$$

Substituting Eq. (53a) into Eq. (50), one obtains the SWVC contribution

$$I_{vc}^{sw} = \frac{4(xx')^2 N_{21}\check{\gamma}_{12}\theta_{23}}{\gamma_3\Gamma_2^t(ku)^2 k'u\,\pi^{1/2}}\sum_{n=1}^{\infty}\sum_{j=1}^{2}\left(\frac{\Gamma_2}{\Gamma_2^t}\right)^n\frac{1}{\sigma_n}$$

$$\times\ \mathrm{Im}\begin{cases} -B_j\left(\frac{ku}{\gamma_B}\right)\int_{-\infty}^{\infty}dx\ \frac{\exp(-x^2)}{r_j - x}\ Z_i\left(\frac{i\gamma_B/ku + \alpha^n x}{\sigma_n}\right) & \text{(5} \\ \text{or} & \\ B_j\int_{-\infty}^{\infty}dx\ \frac{\exp(-x^2)}{|x+i\gamma_B/ku|^2}\ \tilde{Z}\left(\frac{r_j-\alpha^n x}{\sigma_n}\right) & \text{(5} \end{cases}$$

where

$$Z_i(x) = \mathrm{Im}[Z(x)]\ ;\quad Z_r(x) = \mathrm{Re}[Z(x)] \qquad \text{(5}$$

In practice the sum may be terminated at some N for which $\alpha^N \ll 1$, and the sum from n = N to ∞ explicitly evaluated. In this manner the sum from 1 to ∞ may be written

$$\sum_{n=1}^{\infty}\{\ldots\} = \sum_{n=1}^{N-1}\{\ldots\} + \mathrm{Im}\sum_{j=1}^{2}\pi^{1/2}\left(\frac{ku}{\gamma_B}\right)B_j\,\mathcal{R}_N\,\tilde{Z}(r_j)\,Z_i\left(\frac{i\gamma_B}{ku}\right) \qquad \text{(5}$$

where

$$\mathcal{R}_N = \left(\frac{\Gamma_{22}}{\Gamma_2^t}\right)^N\frac{\Gamma_2^t}{\gamma_2} \qquad \text{(56b)}$$

$$\alpha^N \ll 1 \qquad \text{(56c)}$$

with the sum from n = 1 to (N-1) evaluated by numerical integration. Thus, the LAS line shape for the KSK is given by Eqs. (36a, b, d) and (54), and for an arbitrary kernel by Eqs. (36a, b, d), (50), and (49).

IV. Limiting Forms for the Line Shape

It is possible to obtain limiting forms for the line shape in several cases of practical interest. In this section, we give line shape expressions valid for (A) weak-pump-field, (B) large pump detuning, (C) arbitrarily strong pump-field in the Doppler limit and (D) weak-pump-field in the Doppler limit. The results are discussed in Sec. V, where representative line shapes are displayed. Some of these results are not new, but are included for completeness.

A. Weak-Pump-Field

The weak-pump-field limit ($\chi \ll$ all $\tilde{\gamma}$'s) has been treated previously[11], and may also be obtained from Eqs. (35), (36), (50), and (54) by straightforward algebra. To order χ^2 the line shape is given by

$$I_s(\Delta,\Delta') = I^{T\alpha}_{12} + I^{sw}_{nvc} + I^{sw}_{vc} + I^{T\alpha}_{nvc} \tag{57a}$$

$$I^{T\alpha}_{12} \sim -\frac{2(\chi\chi')^2 N_{21}}{\gamma_3\, ku\, k'u\, k''u}\, \mathrm{Im}\; I_2\left(\frac{i\tilde{\gamma}_{23}}{k'u}, \frac{i\tilde{\gamma}_{12}}{ku}, \frac{i\tilde{\gamma}_{13}}{k''u}; \theta_{12}\theta_{23}, \theta_{13}\theta_{23}\right) \tag{57b}$$

$$I^{sw}_{nvc} \sim \frac{2(\chi\chi')^2 N_{21}}{\gamma_3 \Gamma_2^t\, ku\, k'u}\, \mathrm{Re}\left[I_1\left(\frac{i\tilde{\gamma}_{23}}{k'u}, \frac{i\tilde{\gamma}''_{12}}{ku}, -\theta_{12}\theta_{23}\right) + I_1\left(\frac{i\tilde{\gamma}_{23}}{k'u}, \frac{i\tilde{\gamma}_{12}}{ku}, \theta_{12}\theta_{23}\right)\right] \tag{57c}$$

$$I^{sw}_{vc} \sim -\frac{4(\chi\chi')^2\, \tilde{\gamma}_{12}\, \tilde{\gamma}_{23}\, u^6}{\gamma_3 \Gamma_2^t (ku)^2 (k'u)^2} \iint d\vec{x}\, d\vec{y}$$

$$\times \frac{\delta G_2(u\vec{y} \to u\vec{x})\, N_{21}(u\vec{y})}{\left[(\gamma_2/ku)^2 + (y - \theta_{12}\Delta_{12}/ku)^2\right]\left[(\tilde{\gamma}_{23}/k'u)^2 + (x - \theta_{23}\Delta_{23}/k'u)^2\right]}$$

arbitrary kernel (57d)

$$I^{sw}_{vc} \sim -\frac{4(\chi\chi')^2 N_{21}}{\gamma_3 \Gamma_2^t\, ku\, k'u\, \pi^{1/2}} \sum_{n=1}^{\infty} \left(\frac{\Gamma_2}{\Gamma_2^t}\right)^n \frac{1}{\sigma_n}$$

$$\times \begin{cases} \displaystyle\int_{-\infty}^{\infty} dx \left(\frac{\tilde{\gamma}_{23}}{ku}\right) \frac{e^{-x^2}\, Z_i\left[(i\tilde{\gamma}_{12}/ku + \alpha^n x\,\theta_{12})/\sigma_n\right]}{(\tilde{\gamma}_{23}/k'u)^2 + (x - \theta_{23}\Delta_{23}/k'u)^2} \\ \text{or} \\ \displaystyle\int_{-\infty}^{\infty} dx \left(\frac{\tilde{\gamma}_{12}}{ku}\right) \frac{e^{-x^2}\, Z_i\left[(i\tilde{\gamma}_{23}/k'u + \alpha^n x\,\theta_{23})/\sigma_n\right]}{(\tilde{\gamma}_{12}/ku)^2 + (x - \theta_{12}\Delta_{12}/ku)^2} \end{cases}$$

KSK (57d')

$$I^{T\alpha}_{23} \sim \frac{2(\chi\chi')^2 N_{32}}{\gamma_3 (k'u)^2 k''u}\, \mathrm{Im}\; I_3\left(\frac{i\tilde{\gamma}_{23}}{k'u}, \frac{i\tilde{\gamma}_{13}}{k''u}, \theta_{13}\theta_{23}\right) \tag{57e}$$

where the functions I_1, I_2 and I_3 are defined by

$$I_1(\mu_1,\mu_2,\epsilon) = -M(\mu_1,\mu_2,\epsilon)\left[Z(\mu_1) - \epsilon Z(\mu_2)\right] \tag{58a}$$

$$I_2(\mu_1,\mu_2,\mu_3,\epsilon,\epsilon') = M(\mu_1,\mu_2,\epsilon)\left[I_1(\mu_1,\mu_3,\epsilon') - \epsilon I_1(\mu_2,\mu_3,\epsilon/\epsilon')\right] \tag{58b}$$

$$I_3(\mu_1,\mu_2,\epsilon) = -M(\mu_1,\mu_2,\epsilon)\left\{\epsilon I_1(\mu_1,\mu_2,\epsilon) + 2\left[1+\mu_1 Z(\mu_1)\right]\right\} \tag{58c}$$

with

$$M(\mu_1,\mu_2,\epsilon) = \left[\mu_2 - \epsilon\mu_1\right]^{-1} \tag{58d}$$

and $\delta G_2(\vec{v}'\to\vec{v})$ in Eq. (57d) is to be determined from Eq. (49).

B. Large Pump Detuning

In the limit of large pump detuning [$|\Delta| >>$ all γ's, $|\Delta| >> ku$], the SW contribution is greatly simplified. The population density $n_2(\vec{v})$ is proportional to $N_{21}(\vec{v})$ since each velocity subgroup is excited with equal (albeit small) probability by the off-resonant pump field. Collisions do not alter $N_{21}(\vec{v})$; consequently the line shape in this limit is independent of velocity-changing collisions in level 2. The line shape is found to possess resonances in the regions $\Delta_{13} \approx 0$, $\Delta_{23} \approx 0$ and, in the region of these resonances, one finds[11,23]

$$I_3(\Delta,\Delta') \sim \frac{-2(\chi\chi')^2 N_{31}}{\gamma_3 k''u(\Delta_{12})^2} Z_i\left(\frac{i\tilde{\gamma}_{13}}{k''u}\right) \qquad \Delta_{13} \approx 0 \tag{59a}$$

$$\sim -\frac{2(\chi\chi')^2}{\gamma_3 k'u(\Delta_{12})^2}\left\{N_{21}\left(\frac{2\tilde{\gamma}_{12}}{\gamma_2}-1\right)Z_i\left(\frac{i\tilde{\gamma}_{23}}{k'u}\right) + \frac{2N_{32}\Delta_{12}}{k'u}\left[\frac{\Delta_{23}}{k'u}Z_i\left(\frac{i\tilde{\gamma}_{23}}{k'u}\right) - \frac{\tilde{\gamma}_{23}}{k'u}Z_r\left(\frac{i\tilde{\gamma}_{23}}{k'u}\right)\right] - N_{32}\,\theta_{13}\,\theta_{23}(k''/k')\,Z_i(i\tilde{\gamma}_{23}/k'u)\right\} \qquad \Delta_{23} \approx 0 \tag{59b}$$

As has been discussed elsewhere[11,17,24], the line shape includes collisionally aided radiative excitation of level 2. It contains a Doppler broadened resonance at $\Delta' \approx 0$, in addition to the "direct" two quantum resonance (which may be broad or narrow) centered near $\Delta' = -\epsilon\epsilon'\Delta$. In addition, I_{32}^{TQ} contributes a dispersion-like term near $\Delta' \approx 0$. Note that the limits on $|\Delta|$ imply that the large pump detuning case also satisfies the weak pump field criteria.

C. Arbitrarily Strong Pump-Field in the Doppler Limit

The "Doppler limit" refers to the limit in which velocity-selected atoms provide the major contribution to the line shape. This limiting form for the line shape has been examined for arbitrarily strong pump-fields and no collisions[4-7] or for weak-pump-fields including collisions[11], but general expressions including effects of velocity-changing collisions and arbitrarily strong pump-fields have not been previously obtained. The Doppler limit is achieved if <u>both</u> the homogeneous widths are smaller than the Doppler widths, <u>i.e.</u> $\gamma_B << ku$; $\tilde{\gamma}_{23} << k'u$ <u>and</u> the detunings are within the Doppler profiles, <u>i.e.</u> $|\Delta| < ku$; $|\Delta'| < k'u$. In the Doppler limit, only atoms having $v_z' \approx \Delta/k$, $v_z \approx \epsilon\Delta'/k'$ contribute appreciably to the line shape and slowly varying functions of v_z' or v_z, such as the atomic velocity distribution, can be evaluated at these values of v_z' and v_z, respectively.

The Doppler limit expressions are most conveniently calculated from Eqs. (33), (16), (28), and (32) for I_{12}^{TQ}, I_{nvc}^{SW} and I_{23}^{TQ} and from Eqs. (50) and (54) for I_{vc}^{SW}. One obtains the line shape in the Doppler limit for arbitrarily strong pump-fields as

$$I_s(\Delta,\Delta') = I_{12}^{TQ} + I_{nvc}^{SW} + I_{vc}^{SW} + I_{23}^{TQ} \tag{60a}$$

$$I_{12}^{TQ} \sim -\frac{2(\chi\chi')^2 N_{21}\,\theta_{12}\theta_{23}\theta_{13}\,\pi^{1/2}}{\gamma_2\, ku\, k'u\, k''u} \exp\left[-\left(\frac{\Delta_{12}}{ku}\right)^2\right] \mathrm{Re}\sum_{j=1}^{4}\theta_j A_j \tag{60b}$$

$$I_{nvc}^{SW} \sim \frac{4(\chi\chi')^2 N_{21}\,\tilde{\gamma}_{12}\,\theta_{23}\,\pi^{1/2}}{\gamma_2 \Gamma_2^2 (ku)^2 k'u} \exp\left[-\left(\frac{\Delta_{12}}{ku}\right)^2\right] \mathrm{Re}\sum_{j=1}^{4}\theta_j D_j \tag{60c}$$

$$I_{vc}^{SW} \sim \frac{4(\chi\chi')^2 N_{21}\,\tilde{\gamma}_{12}\,\theta_{23}}{\gamma_2 \Gamma_2^2 (ku)^2 k'u\, \pi^{1/2}} \exp\left[-\left(\frac{\Delta_{12}}{ku}\right)^2\right]$$

$$\times \mathrm{Im}\begin{cases} u\iint_{-\infty}^{\infty} dx\,dy\, \dfrac{\delta G_{22}(uy \to ux)(x-\lambda_1)}{(x-\lambda_1)(x-\lambda_2)(x-\lambda_3)(x-\lambda_4)} & \text{arbitrary kernel} \quad (60d) \\ \displaystyle\sum_{j=1}^{2}\sum_{n=1}^{\infty}\int_{-\infty}^{\infty} dy\, B_j \left(\frac{\Gamma_2}{\Gamma_2^2}\right)^n \frac{1}{\sigma_n}\, \frac{\tilde{Z}\left[(\lambda_j - \alpha^n y)/\sigma_n\right]}{(\gamma_B/ku)^2 + (y - \Delta_{12}\theta_{12}/ku)^2} & \text{KSK} \quad (60d') \end{cases}$$

$$I_{23}^{TQ} \sim \frac{2(\chi')^2 N_{22}\,\theta_{23}\,\pi^{1/2}}{\gamma_3\, k'u} \exp\left[-\left(\frac{\Delta_{23}}{k'u}\right)^2\right] \mathrm{Re}\left[\sum_{j=1}^{2}\theta_j B_j + \theta_{23}\right] \tag{60e}$$

where

$$\delta G_{22}(v_z' \to v_z) = \iiiint_{-\infty}^{\infty} dv_x\,dv_y\,dv_x'\,dv_y'\,(\pi u^2)^{-1} \times \exp\{-[(v_x')^2 + (v_y')^2]/u^2\}\,\delta G_2(\vec{v}' \to \vec{v}) \tag{61}$$

$$\theta_j = \mathrm{SGN}[\mathrm{Im}(\lambda_j)] \tag{62a}$$

$$\mathrm{SGN}(x) = \begin{cases} +1 & x>0 \\ -1 & x<0 \end{cases} \tag{62b}$$

Owing to Eqs. (44), it appears that I_{12}^{TQ} and I_{nvc}^{SW} can vanish if all the θ_j are equal. However, it follows from Eqs. (62) and (37c,d) that $\theta_3 = -\theta_4$; consequently I_{12}^{TQ} and I_{nvc}^{SW} are both non-zero in the strong pump-field-Doppler limit for <u>arbitrary</u> level schemes (<u>i.e.</u> arbitrary B,B',c). The fact that I_{12}^{TQ} does <u>not</u> vanish in the Doppler limit for level schemes corresponding to $\theta_{12}\theta_{23} = 1$ is unique to the strong field case; as is well known[1-8,11] it vanishes in the weak-field Doppler limit under such conditions. On the other hand, for strong pump fields (but not so strong that the Doppler limit is violated), I_{23}^{TQ} is small if $\theta_1 = \theta_2 = -\theta_{23}$, as is the case in the weak-field-Doppler limit.

A further reduction of Eqs. (60d,d') is possible if the <u>kernel</u> is also a slowly varying function of velocity compared with the hole width γ_B/k; <u>i.e.</u> if $k(\Delta u) \gg \gamma_B$ (note, our LAS model already requires $k(\Delta u) > \gamma_B$). In that limit, the Im$\{$ ... terms in Eqs. (60d, d') become

$$\mathrm{Im}\{\cdots = \mathrm{Im}\begin{cases} \pi \dfrac{ku}{\gamma_B}\, u \displaystyle\int_{-\infty}^{\infty} dx\, \frac{\delta G_{22}(\Delta_{12}\theta_{12}/k \to xu)(x-\lambda_1)}{(x-\lambda_1)(x-\lambda_2)} & \text{arbitrary kernel} \quad (60f) \\ \pi \dfrac{ku}{\gamma_B} \displaystyle\sum_{j=1}^{2}\sum_{n=1}^{\infty} B_j \left(\frac{\Gamma_2}{\Gamma_2^2}\right)^n \frac{1}{\sigma_n}\, \tilde{Z}\left(\frac{\lambda_j - \alpha^n \Delta_{12}\theta_{12}/ku}{\sigma_n}\right) & \text{KSK} \quad (60f') \end{cases}$$

Moreover, if the kernel width Δu is also large compared with $\tilde{\gamma}_{23}/k'$ and $\tilde{\gamma}_{13}/k''$, this contribution further reduces to

$$\mathcal{I}m\left\{ \cdots \right. = \mathcal{I}m\left\{ \pi^{3/2}\frac{ku}{\gamma_B}\sum_{j=1}^{2} B_j\theta_j \begin{bmatrix} \pi^{1/2}u\,\delta G_{2+}\left(u\Delta_{12}\theta_{12}/k \to u\,Re(\kappa_j)\right) \\ \text{arbitrary kernel} \\ (\Gamma_2/\Gamma_2^c)^n\sigma_n^{-1}\exp -\left[\frac{Re(\kappa_j)-\alpha^n\Delta_{12}\theta_{12}/ku}{\sigma_n}\right]^2_{\text{KSK}} \end{bmatrix} \right. \qquad \begin{matrix} (60g) \\ \\ (60g') \end{matrix}$$

D. Weak-Pump-Field in the Doppler Limit

If both the limits discussed in subsections (A) and (C) above are applicable, Eqs. (57) take the familiar form[1-8,11]

$$I_s(\Delta,\Delta') = I_{12}^{TA} + I_{nvc}^{SW} + I_{vc}^{SW} + I_{23}^{TA} \qquad (63a)$$

$$I_{12}^{TA} \sim -\frac{4(\kappa\kappa')^2 N_{21}\pi^{1/2}}{\gamma_3\,ku\,k'u\,k''u}\exp\left[-\left(\frac{\Delta_{12}}{ku}\right)^2\right]\left\{\frac{\tilde{\eta}_a^R\tilde{\eta}_b^R-\tilde{\eta}_a^I\tilde{\eta}_b^I}{|\tilde{\eta}_a|^2|\tilde{\eta}_b|^2}\delta_{\theta_{13}\theta_{23},-1}\right.$$

$$\left. + \frac{\tilde{\eta}_a^R\tilde{\eta}_c^R-\tilde{\eta}_a^I\tilde{\eta}_c^I}{|\tilde{\eta}_a|^2|\tilde{\eta}_c|^2}\delta_{\theta_{13}\theta_{12},-1}\right\}\delta_{\theta_{12}\theta_{23},-1} \qquad (63b)$$

$$I_{nvc}^{SW} \sim -\frac{4(\kappa\kappa')^2 N_{21}\pi^{1/2}}{\gamma_3\Gamma_2^c\,ku\,k'u}\exp\left[-\left(\frac{\Delta_{12}}{ku}\right)^2\right]\frac{\tilde{\eta}_a^R}{|\tilde{\eta}_a|^2} \qquad (63c)$$

$$I_{vc}^{SW} \sim -\frac{4(\kappa\kappa')N_{21}}{\gamma_3\Gamma_2^c\,ku\,k'u\,\pi^{1/2}}\exp\left[-\left(\frac{\Delta_{12}}{ku}\right)^2\right]$$

$$\times\left\{\begin{matrix} \dfrac{\tilde{\gamma}_{23}}{k'u}u\displaystyle\iint_{-\infty}^{\infty}dx\,dy\frac{\delta G_{22}(uy\to ux)}{[(\tilde{\gamma}_{23}/k'u)^2+(x-\theta_{13}\Delta_{23}/k'u)^2][(\tilde{\gamma}_{12}/ku)^2+(y-\theta_{12}\Delta_{12}/ku)^2]} \\ \text{arbitrary kernel} \\ \displaystyle\sum_{n=1}^{\infty}(\Gamma_2/\Gamma_2^c)^n\sigma_n^{-1}\int_{-\infty}^{\infty}dy\frac{Z_i(i\tilde{\gamma}_{23}/k'u+\alpha^n\theta_{23}y)}{(\tilde{\gamma}_{12}/ku)^2+(y-\Delta_{12}\theta_{12}/ku)^2}\ \text{KSK} \end{matrix}\right. \qquad \begin{matrix} (63d) \\ \\ (63d') \end{matrix}$$

$$I_{23}^{TA} = \frac{4(\kappa\kappa')^2 N_{32}\pi^{1/2}}{\gamma_3(k'u)^2\,k''u}\exp\left[-\left(\frac{\Delta_{12}}{ku}\right)^2\right]\frac{\left[(\tilde{\eta}_b^R)^2-(\tilde{\eta}_b^I)^2\right]}{|\tilde{\eta}_b|^4}\delta_{\theta_{13}\theta_{23},-1} \qquad (63e)$$

where

$$\tilde{\eta}_{a,b,c}^R = Re\,\tilde{\eta}_{a,b,c}\ ; \quad \tilde{\eta}_{a,b,c}^I = \mathcal{I}m\,\tilde{\eta}_{a,b,c} \qquad (64a)$$

$$\tilde{\eta}_a^R = \frac{\tilde{\gamma}_{23}}{k'u}+\frac{\tilde{\gamma}_{12}}{ku}\ ; \quad \tilde{\eta}^I = \frac{\Delta_{23}}{k'u} - SGN(\theta_{12}\theta_{13})\frac{\Delta_{12}}{ku} \qquad (64b)$$

$$\tilde{\eta}_b = \frac{\eta_{13}}{k''u}+\frac{\eta_{23}}{k'u} \qquad (64c)$$

$$\tilde{\eta}_c = \frac{\eta_{13}}{k''u}+\frac{\eta_{12}}{ku} \qquad (64d)$$

If $k(\Delta u) > \gamma_B$, the $\{\ldots$ terms in Eqs. (63d, d') become

$$\left\{\cdots = \pi \frac{ku}{\tilde{\gamma}_{12}} \begin{cases} \dfrac{\tilde{\gamma}_{23}u}{k'u} \displaystyle\int_{-\infty}^{\infty} dx \; \underbrace{\dfrac{\delta G_{2a}(\Delta_{12}\theta_{12}/k \to ux)}{(\tilde{\gamma}_{23}/k'u)^2 + (x - \Delta_{23}\theta_{23}/k'u)^2}}_{\text{arbitrary kernel}} & (63f) \\ \sum_{n=1}^{\infty} (\Gamma_2/\Gamma_2^t)^n \sigma_n^{-1} Z_i\left[(i\tilde{\gamma}_{13} + \alpha^n \theta_{12}\theta_{23}\Delta_{12} k'/k)/(k'u\sigma_n)\right] & \text{KSK} \quad (63f') \end{cases}\right.$$

and if, in addition, $k'\Delta u > \tilde{\gamma}_{23}$, they reduce to

$$\left\{\cdots = \pi^{3/2} \frac{ku}{\tilde{\gamma}_{12}} \begin{cases} \pi^{1/2} u \; \underbrace{\delta G_{2a}(\Delta_{12}\theta_{12}/k \to \Delta_{23}\theta_{23}/k')}_{\text{arbitrary kernel}} & (63g) \\ \sum_{n=1}^{\infty} (\Gamma_2/\Gamma_2^t)^n \sigma_n^{-1} \exp\left[-\left(\dfrac{\Delta_{23} - \alpha^n \theta_{12}\theta_{23}\Delta_{12} k'/k}{k'u\sigma_n}\right)^2\right] & \text{KSK} \quad (63g') \end{cases}\right.$$

V. Representative Line Shapes

In this section, a few representative probe absorption line profiles are displayed and discussed. Results are always given with either $N_{32} = 0$ (giving $I_{12}^{TQ} + I_{nvc}^{SW} + I_{vc}^{SW}$, the probe absorption proportional to N_{21}) or $N_{21} = 0$ (giving I_{23}^{TQ}, the probe absorption proportional to N_{32} with the linear probe absorption subtracted out). One must add the $N_{32}=0$ and $N_{21} = 0$ contributions, properly weighted, to characterize the most general experimental situation, in which $N_{32} \neq 0$, $N_{21} \neq 0$. In all cases, we take $\gamma_1 = 0$, $\gamma_2' = \gamma_2$, $\beta = \beta' = 1$ to simulate an upward cascade in which level 1 is the ground state.[25] Unless noted otherwise the following parameters are used

$N_{21} = -1$, $N_{32} = 0$ or $N_{32} = -1$, $N_{21} = 0$

$\gamma_1 = 0$, $\gamma_2 = .02$, $\gamma' = .02$, $\gamma_3 = .01$

$\tilde{\gamma}_{12} = .01 + .007\ P$

$\tilde{\gamma}_{23} = .015 + .015\ P$

$\tilde{\gamma}_{13} = .005 + .016\ P$

$S_{12}^{ph} = S_{23}^{ph} = S_{13}^{ph} = 0$

$k'/k = 0.4$

$\Gamma_1 = .004\ P$; $\Gamma_2 = .006\ P$

All frequencies are given in units of (ku) and P is the pressure in Torr. These parameters are typical of atom-atom collisions when levels 1, 2, and 3 are different electronic states. By restricting the discussion to $k'/k < 1$, we are omitting some interesting effects[4-7] (vanishing of I_{23}^{TQ} for weak fields, modification of line splitting in strong fields). The ratio $k'/k = 0.4$ is chosen to enhance the visibility of ac Stark splittings.[7]

Velocity-changing collisions are described by a KSK with

$$\alpha = 0.4 \; ; \; \tilde{u} = 0.93u,$$

which corresponds roughly to hard-sphere large-angle scattering by atoms of equal mass. The only remaining parameters to specify are Δ, ϵ, P and χ. The line shape $I_s(\Delta,\Delta')$, normalized to χ^2, is then displayed in the same arbitrary units.

In Fig. 2, the Doppler limit line shapes with $N_{32} = 0$ are shown as a function of χ for co- ($\epsilon = 1$, broken line) and counter- ($\epsilon = -1$, solid line) propagating fields, $\Delta = -1$ and $P = 0$. For counterpropagating fields, at low field strengths, the line is a narrow Lorentzian centered at $\Delta' = \epsilon(k'/k)\Delta = 0.4$ with a HWHM of η_b^R; as the field strength χ is increased such that $\chi > \gamma_{ij}$, the line splits owing to the ac Stark effect.[1-8] For copropagating fields and $\chi << \gamma$'s, the line is a Lorentzian centered at $\Delta' = \epsilon(k'/k)\Delta = -0.4$ with a HWHM of η_a^R that is greater than that of the $\epsilon = -1$ case (there is some Doppler phase cancellation for counter-propagating fields). For sufficiently large χ, the $\epsilon = 1$ line shape also exhibits ac Stark splitting. This splitting effect, which was also noted in Ref. 4, is dependent on the fact that $\gamma_2' \approx \gamma_2$; it vanishes if branching to level 1 is negligible ($\gamma_2' << \gamma_2$).

The $N_{21} = 0$ Doppler-limit line shape is shown in Fig. 3 as a function of χ for $P = 0$, $\Delta = -1$ and $\epsilon = -1$. The line shapes shown with $\chi = 1.0\times10^{-4}$ and $\chi = .01$ are typical for the case $\chi << ku$ which has been discussed by previous authors.[2-8] The $\chi = 0.2$ line shape indicates a new feature characteristic of the case $\chi \gtrsim ku$. In this strong-field limit, I_{23}^{TQ} (i.e. - component of $I_s(\Delta,\Delta') \propto N_{32}$) may be thought to consist of two

parts. First there is an ac Stark split profile, similar to I_{nvc}^{SW} of the $N_{32} = 0$ case giving the total probe absorption. Then there is the linear absorption component that must be subtracted off to give the saturation spectroscopy profile. The linear absorption appears as the negative part of the line shape between the two peaks. As is easily derived, $\int I_{23}^{TQ}(\Delta,\Delta')d\Delta' = 0$.

The case of large detuning, $\Delta = -10$, is depicted in Figs. 4 and 5 for counter-propagating waves [see Eqs. (59)]. In Fig. 4, $N_{32} = 0$ and results are plotted as a function of P for $\chi = 0.01$. There is always a "direct" two-quantum resonance centered at $\Delta' = -\Delta = 10$. This component is Doppler broadened, since $k''u = (k - k')u = 0.6$. In addition, there is the broad collisional redistribution term centered at $\Delta' = 0$ which increases with increasing P and vanishes for $P = 0$ (the vanishing at $P = 0$ is a consequence of taking $\gamma_1 = 0$). We have recently undertaken a systematic experimental study of this effect and found good agreement with theory.[17]

In Fig. 5, $N_{21} = 0$ and one sees the dispersion-like contribution of I_{23}^{TQ}, centered near $\Delta' = 0$, predicted by Eq. (59). With increasing pressure this contribution broadens somewhat. Note that, for $\Delta = -10$, the amplitude of the dispersion term is 30 times that from the "direct" transition.

The effect of velocity-changing collisions is seen in Figs. 6 and 7 for weak and strong pump fields, respectively, with $\Delta = -1$, $\epsilon = -1$. With increasing pressure, the population density $n_2(\vec{v})$ approaches an

equilibrium distribution and the corresponding probe absorption approaches a Voigt profile centered at $\Delta' = 0$. By monitoring the line shape as a function of pressure, one can obtain information on the collision kernel giving rise to the velocity-changing collisions.

Figure 6 is applicable to the weak-pump field limit.[11] Velocity-changing collisions remove atoms from the velocity bump created by the pump field, leading to absorption over an increased range of probe frequencies. The integrated line shape remains constant.

Figure 7 illustrates two interesting features of collision effects in strong-pump-field saturation spectroscopy. First, the integrated probe absorption, which is proportional to $\tilde{\gamma}_{12}/\gamma_B$, grows with increasing perturber pressure; it would saturate at $\tilde{\gamma}_{12} \gtrsim \chi$ ($\gamma_B \approx \tilde{\gamma}_{12}$). Second, the peak probe absorption also begins to increase for sufficiently high perturber pressure. Probe absorption from the excited state velocity distribution becomes more efficient since collisions (a) increase the pump absorption and (b) redistribute atoms into a velocity range where they can interact more effectively with the probe. Although not displayed, the corresponding integrated and peak probe absorption for $\chi = .2$, $\Delta = -1$, $\epsilon = 1$ also increase with increasing perturber pressure. (The splitting seen in Fig. 2 disappears at low perturber pressures). Thus, to maximize probe absorption, as is desirable in laser isotope separation schemes, one should use perturber pressures that give $\tilde{\gamma}_{12} \approx \chi$ (provided that any quenching channels are not enhanced by collisional effects).

VI. Summary

We have presented a theory of saturation spectroscopy in three-level systems, including collisional effects. Using a model of collisions in which they are phase-interrupting in their effect on level coherences and velocity-changing in their effect on level population densities, we have calculated the probe absorption line shape in the presence of a strong pump field acting on a coupled transition. Line shapes for such systems enable one to extract data concerning the collision kernels and rates giving rise to the scattering effects. Specific results were obtained for a Keilson-Storer kernel in the large-angle scattering limit. An analysis of foreign gas broadening of the saturation spectroscopy line shape of Na $3S_{1/2} \to 3P_{1/2} \to 4D_{3/2}$, based on the above theory, is presented in other papers.[17]

This research was supported in part by the U.S. Office of Naval Research. One of us (P.R.B.) would like to thank Dr. J. Lam, M. J.L. LeGouët and Drs. S.D. Yeh and E.J. Robinson for helpful discussions concerning this problem.

Appendix

In this appendix, the theory is extended to include a situation often encountered experimentally, an inelastic collisional decay channel for level 2. That is, we assume that level 2 is collisionally coupled to a new level [denoted by "4"]. Level 4 may spontaneously decay to the ground state with some rate γ_4'. However, it is assumed that level 4 is sufficiently separated in energy from level 2 that one can neglect field-induced transitions between levels 1 and 4 and levels 4 and 3 for the external field frequencies under consideration which are in near resonance with the 1-2 and 2-3 transition frequencies, respectively. There will be probe absorption near ω_{34} but this is a separate effect that is well separated from probe absorption near ω_{32}.

The 2-4 collisional coupling may be incorporated into the problem by the addition of the following terms to the rhs of the equation indicated

$$(10a) \qquad \gamma_4' \tilde{\rho}_{44}(\vec{v}) \tag{A1a}$$

$$(10b) \qquad -\Gamma_{24}(\vec{v})\tilde{\rho}_{22}(\vec{v}) + \int d\vec{v}'\, W_{42}(\vec{v}'\to\vec{v})\tilde{\rho}_{22}(\vec{v}') \tag{A1b}$$

where $W_{ij}(\vec{v}'\to\vec{v})$ is the inelastic kernel for $i \to j$ collisional coupling and $\Gamma_{ij}(\vec{v})$ is the rate for $i \to j$ collisions. One must also add the following equation for the population density of level 4

$$\Gamma_4^t(\vec{v})\tilde{\rho}_{44}(\vec{v}) = \int d\vec{v}'\, W_4(\vec{v}'\to\vec{v})\tilde{\rho}_{44}(\vec{v}') - \Gamma_{42}(\vec{v})\tilde{\rho}_{44}(\vec{v}) + \int d\vec{v}'\, W_{24}(\vec{v}')\tilde{\rho}_{22}(\vec{v}') + \lambda_4(\vec{v}) \tag{A2}$$

It is assumed that collisions can not create any coherence between level 4 and any of the other levels - i.e. $\tilde{\rho}_{4j} = 0$ for $j \neq 4$.

The line shape is still given by Eqs. (33), (16), (28) with $n_2(\vec{v})$ and $\rho_{12}^{(0)}(\vec{v})$ determined from the equations

$$\Gamma_1^t(\vec{v})\, n_1(\vec{v}) = \int d\vec{v}'\, W_1(\vec{v}'\to\vec{v})\, n_1(\vec{v}') + i\chi\left[\tilde{\rho}_{21}^{(0)}(\vec{v}) - \tilde{\rho}_{12}^{(0)}(\vec{v})\right] + \gamma_2'\, n_2(\vec{v}) + \gamma_4'\, n_4(\vec{v}) \tag{A3a}$$

$$\Gamma_2^t(\vec{v})\, n_2(\vec{v}) = \int d\vec{v}'\, W_2(\vec{v}'\to\vec{v})\, n_2(\vec{v}') - i\chi\left[\tilde{\rho}_{21}^{(0)}(\vec{v}) - \tilde{\rho}_{12}^{(0)}(\vec{v})\right] - \Gamma_{24}(\vec{v})\, n_2(\vec{v}) + \int d\vec{v}'\, W_{42}(\vec{v}'\to\vec{v})\, n_4(\vec{v}') \tag{A3b}$$

$$\Gamma_4^t(\vec{v})\, n_4(\vec{v}) = \int d\vec{v}'\, W_4(\vec{v}'\to\vec{v})\, n_4(\vec{v}') - \Gamma_{42}(\vec{v})\, n_4(\vec{v}) + \int d\vec{v}'\, W_{24}(\vec{v}'\to\vec{v})\, n_2(\vec{v}') \tag{A3c}$$

$$\mu_{12}(\vec{v})\,\tilde{\rho}_{12}^{(0)}(\vec{v}) = i\chi\left[N_{21}(\vec{v}) + n_2(\vec{v}) - n_1(\vec{v})\right] \tag{A3d}$$

$$\tilde{\rho}_{21}^{(0)}(\vec{v}) = \left[\tilde{\rho}_{12}^{(0)}(\vec{v})\right]^* \tag{A3e}$$

$$N_{ij}(\vec{v}) = N_i(\vec{v}) - N_j(\vec{v}) \tag{A3f}$$

where the $N_i(\vec{v})$ are the equilibrium population densities in the absence of external fields. The $N_i(\vec{v})$ are defined as solutions to

$$\Gamma_1^e(\vec{v})\, N_1(\vec{v}) = \int d\vec{v}'\, W_1(\vec{v}'\to\vec{v})\, N_1(\vec{v}') + \gamma_2' N_2(\vec{v}) + \gamma_4' N_4(\vec{v}) + \lambda_1(\vec{v}) \tag{A4a}$$

$$\Gamma_2^e(\vec{v})\, N_2(\vec{v}) = \int d\vec{v}'\, W_2(\vec{v}'\to\vec{v})\, N_2(\vec{v}') - \Gamma_{24} N_2(\vec{v}) + \int d\vec{v}'\, W_{42}(\vec{v}')\, N_4(\vec{v}') + \lambda_2(\vec{v}) \tag{A4b}$$

$$\Gamma_4^e(\vec{v})\, N_4(\vec{v}) = \int d\vec{v}'\, W_4(\vec{v}'\to\vec{v})\, N_4(\vec{v}') - \Gamma_{42}(\vec{v}) N_4(\vec{v}) + \int d\vec{v}'\, W_{24}(\vec{v}'\to\vec{v})\, N_2(\vec{v}') + \lambda_4(\vec{v}) \tag{A4c}$$

$$N_3(\vec{v}) = \lambda_3(\vec{v})/\gamma_3 \tag{A4d}$$

Equations (A3) must, in general, be solved numerically once the kernels are specified.

There is, however, a limiting case of some practical interest for which analytic solutions of Eqs. (A3) may be found. If the energy separation of levels 2 and 4 is $<0.1x$ (thermal energy), then collisions can transfer population between levels 2 and 4 without resulting in a significant velocity change. We consider such a case, for which

$$W_{42}(\vec{v}'\to\vec{v}) = \Gamma_{42}(\vec{v})\,\delta(\vec{v}-\vec{v}')\ ; \quad W_{24}(\vec{v}'\to\vec{v}) = \Gamma_{24}(\vec{v})\,\delta(\vec{v}-\vec{v}') \tag{A5}$$

Furthermore, we neglect the velocity dependence of all γ's, adopt the same Keilson-Storer kernel [Eq. (51)] for velocity-changing collisions in levels 2 and 4, assume that the $N_i(\vec{v})$ are Maxwellians with most probable speeds u, and take $\gamma_4 = \gamma_2$, $\gamma_4' = \gamma_2'$. In this limit Equations (A3) for $n_2(\vec{v})$, $n_4(\vec{v})$ and $\rho_{12}^{(0)}(\vec{v})$ reduce to

$$\Gamma_1^e n_1(\vec{v}) - \int d\vec{v}'\, W_1(\vec{v}'\to\vec{v})\, n_1(\vec{v}') = [2\chi^2 \tilde{\gamma}_{12}/R_E(\vec{v})^2](1-\gamma_2'/\Gamma_2^e)[N_{21}(\vec{v}) + \tilde{F}_E(\vec{v})] + (\gamma_2'/\Gamma_2^e)\int d\vec{v}'\, W_2(\vec{v}'\to\vec{v})[n_2(\vec{v}') + n_4(\vec{v}')] \tag{A6a}$$

$$\Gamma_2^e n_2(\vec{v}) - \int d\vec{v}'\, W_2(\vec{v}'\to\vec{v})\, n_2(\vec{v}') = -[2\chi^2 \tilde{\gamma}_{12}/R_E(\vec{v})^2][N_{21}(\vec{v}) + \tilde{F}_E(\vec{v})] - \Gamma_{24} n_2(\vec{v}) + \Gamma_{42}\, n_4(\vec{v}) \tag{A6b}$$

$$\Gamma_2^e n_4(\vec{v}) - \int d\vec{v}'\, W_2(\vec{v}'\to\vec{v})\, n_4(\vec{v}') = -\Gamma_{42} n_4(\vec{v}) + \Gamma_{24} n_2(\vec{v}) \tag{A6c}$$

$$\tilde{\rho}_{12}^{(0)}(\vec{v}) = [i\chi\mu_{12}^{*}(\vec{v})/R_E(\vec{v})^2][N_{21}(\vec{v}) + \tilde{F}_E(\vec{v})] \tag{A6d}$$

where

$$N_i(\vec{v}) = N_i\,(\pi u^2)^{-3/2} \exp(-v^2/u^2) \tag{A7}$$

$$\lambda_i(\vec{v}) = \lambda_i\,(\pi u^2)^{-3/2} \exp(-v^2/u^2) \tag{A8}$$

$$N_1 = [(\lambda_2+\lambda_4)(\gamma_2'/\gamma_2) + \lambda_1]/\gamma_1 \tag{A9a}$$

$$N_2 = [(\lambda_2+\lambda_4)(\Gamma_{42}/\gamma_2) + \lambda_2]/(\gamma_2 + \Gamma_{42} + \Gamma_{24}) \tag{A9b}$$

$$N_3 = \lambda_3/\gamma_3 \tag{A9c}$$

$$R_E(\vec{v})^2 = \gamma_E^2 + (\Delta_{12} - kv_z)^2 \tag{A10a}$$

$$\gamma_E = \tilde{\gamma}_{12}\,[1 + \mathcal{S}_E]^{1/2} \tag{A10b}$$

$$\mathcal{S}_E = \frac{2\chi^2}{\tilde{\gamma}_{12}}\left[\frac{1}{\Gamma_2^E} + \frac{1}{\Gamma_1^e}\left(1 - \frac{\gamma_2'}{\Gamma_2^e}\right)\right] \tag{A10c}$$

$$\Gamma_E = \Gamma_2^e \Gamma_2^T/(\Gamma_2^e + \Gamma_{42}) \tag{A11}$$

$$\Gamma_2^T = \Gamma_2^e + \Gamma_{42} + \Gamma_{24} \tag{A12}$$

$$\tilde{F}_E(\vec{v}) = \frac{1}{\Gamma_2^E}\int d\vec{v}'\, W_2(\vec{v}'\to\vec{v})\left[n_2(\vec{v}') + \frac{\Gamma_{42}}{\Gamma_2^e + \Gamma_{42}}\, n_4(\vec{v}')\right] - [\gamma_2'/(\Gamma_1^e\Gamma_2^e)]\int d\vec{v}'\, W_2(\vec{v}'\to\vec{v})[n_2(\vec{v}') + n_4(\vec{v}')] - (1/\Gamma_1^e)\int d\vec{v}'\, W_1(\vec{v}'\to\vec{v})\, n_1(\vec{v}') \tag{A13}$$

The only difference between Eqs. (21) and Eqs. (A6) is that R_2 is replaced by R_E, F by F_E, and $n_2(\vec{v})$ is determined from the coupled Eqs. (A6b,c) rather than from Eq. (21a). Defining

$$n(\vec{v}) = n_1(\vec{v}) + n_4(\vec{v}) \tag{A14}$$

and dropping the F_E term (LAS limit), one can rewrite Eqs. (A6b,c) in the form

$$\Gamma_2^T n_2(\vec{v}) - \int d\vec{v}'\, W_2(\vec{v}'\to\vec{v})\, n_2(\vec{v}') = A_E(\vec{v}) + \Gamma_{42} n(\vec{v}) \tag{A15a}$$

$$\Gamma_2^E n(\vec{v}) - \int d\vec{v}'\, W_2(\vec{v}'\to\vec{v})\, n(\vec{v}') = A_E(\vec{v}) \tag{A15b}$$

where

$$A_E(\vec{v}) = -\left[2\chi^2 \tilde{\gamma}_{12} / R_E(v)^2\right] N_{21}(\vec{v}) \tag{A16}$$

and Γ_2^T is defined by Eq. (A12). To arrive at results analogous to those of Secs. III and IV, we set

$$n_2(\vec{v}) = n_{2E}^{(0)}(\vec{v}) + \delta n_{2E}(\vec{v}) \;;\; n(\vec{v}) = n_E^{(0)}(\vec{v}) + \delta n_E(\vec{v}) \tag{A17}$$

$$n_{2E}^{(0)}(\vec{v}) = A_E(\vec{v})/\Gamma_2^E \;;\; n_E^{(0)}(\vec{v}) = A_E(\vec{v})/\Gamma_2^E \tag{A18}$$

where δn_{2E} and δn_E satisfy the following equations:

$$\Gamma_2^T \delta n_2^E(\vec{v}) - \int d\vec{v}'\, W_2(\vec{v}'\to\vec{v})\, \delta n_2(\vec{v}')$$
$$= \int d\vec{v}'\, W_2(\vec{v}'\to\vec{v})\, n_{2E}^{(0)}(\vec{v}') + \Gamma_{42}\, \delta n_E(\vec{v}) \tag{A19a}$$

$$\Gamma_2^E \delta n_E(\vec{v}) - \int d\vec{v}'\, W_2(\vec{v}'\to\vec{v})\, \delta n_E(\vec{v}') = \int d\vec{v}'\, W_2(\vec{v}'\to\vec{v})\, n_E^{(0)}(\vec{v}') \tag{A19b}$$

As in Eq. (A8), we can introduce propagators defined by

$$\begin{Bmatrix} \delta n_2^E(\vec{v}) \\ \delta n(\vec{v}) \end{Bmatrix} = \int d\vec{v}' \begin{Bmatrix} \delta G_2^E(\vec{v}'\to\vec{v})\, n_{2E}^{(0)}(\vec{v}') \\ \delta G^E(\vec{v}'\to\vec{v})\, n_E^{(0)}(\vec{v}') \end{Bmatrix} \tag{A20}$$

which satisfy

$$\Gamma_2^T \delta G_2^E(\vec{v}'\to\vec{v}) - \int d\vec{v}''\, W_2(\vec{v}''\to\vec{v})\, \delta G_2^E(\vec{v}'\to\vec{v}'')$$
$$= W_2(\vec{v}'\to\vec{v}) + (\Gamma_{42}\Gamma_E/\Gamma_2^E)\,\delta G^E(\vec{v}'\to\vec{v}) \tag{A21a}$$

$$\Gamma_2^E \delta G^E(\vec{v}'\to\vec{v}) - \int d\vec{v}''\, W_2(\vec{v}''\to\vec{v})\, \delta G^E(\vec{v}'\to\vec{v}'') = W_2(\vec{v}'\to\vec{v}) \tag{A21b}$$

We can now take over all of the equations of the text in Secs. III and IV [Eqs. (35) ff] if the following substitutions are made:

$$\eta_s \to \eta_\varepsilon = \gamma_\varepsilon + i\Delta_{12}$$

$$\mathcal{S} \to \mathcal{S}_\varepsilon$$

$$\gamma_s \to \gamma_\varepsilon$$

$$\delta n_2(\vec{v}) \to \delta n_2^\varepsilon(\vec{v})$$

$$\Gamma_2^t \to \Gamma_2^\varepsilon \quad \text{except in factors} \quad \gamma_2'/\Gamma_2^\varepsilon,\ (\Gamma_2/\Gamma_2^t)^n \tag{A22}$$

$$\delta G_2(\vec{v}'\to\vec{v}) \to \delta G_2^\varepsilon(\vec{v}'\to\vec{v})$$

$$(\Gamma_2/\Gamma_2^t)^n \to (\Gamma_2/\Gamma_2^t)^n f_n$$

where

$$f_0 = 1\ ; \quad f_n = \left[\frac{\Gamma_{42}\Gamma_2^\varepsilon}{\Gamma_2^T\Gamma_2^t} + \frac{\Gamma_2^t}{\Gamma_2^T} f_{n-1}\right] \quad n > 1$$

$$R_N \to \left(\frac{\Gamma_2}{\Gamma_2^t}\right)^N \frac{\Gamma_2^T}{\gamma_2+\Gamma_{42}+\Gamma_{24}}\left[\frac{\Gamma_{42}\Gamma_2^\varepsilon}{\gamma_2\Gamma_2^T} + \frac{\Gamma_2^t}{\Gamma_2^T} f_{N-1}\right]$$

With the above substitutions, the equations of the text are generalized to allow for coupling between states 2 and 4 produced by inelastic collisions. Velocity-changing collisions occur in both levels 2 and 4 (characterized by the same collision kernel), but the collisionally induced transfers 2 ↔ 4 occur without significant change of velocity. Such a model has been recently used to explain the saturation spectroscopy of Na - rare gas systems for the $3S_{1/2} \to 3P_{1/2} \to 4D_{3/2}$ upward cascade.[17] In that system, level "4" is the $3P_{3/2}$ state which is collisionally coupled to $3P_{1/2}$. A discussion of the importance of accounting for the $P_{1/2} \leftrightarrow P_{3/2}$ coupling is given in Ref. 17.

References

1. G.E. Notkin, S.G. Rautian and A.A. Feoktistov, Zh. Eksp. Teor. Fiz. 52, 1673 (1967) [Sov. Phys.- JETP 25, 1112 (1967)].
2. M.S. Feld and A. Javan, Phys. Rev. 177, 540 (1969).
3. T.W. Hänsch and P.E. Toschek, Z. Phys. 236, 213 (1970).
4. T.Y. Popova, A.K.Popov, S.G. Rautian and R.I. Sokolovskii, Zh. Eksp. Teor. Fiz. 57, 850, (1969). [Sov. Phys. - JETP 30, 466, 1208 (1970)].
5. B.J. Feldman and M.S. Feld, Phys. Rev. A5, 899 (1972); N. Skribanowitz, M.J. Kelly and M.S. Feld, Phys. Rev. A6, 2302 (1972).
6. I.M. Beterov and V.P. Chebotaev, Prog. Quantum Elec. 3, 1 (1974) and references therein.
7. R. Salomaa and S. Stenholm, J. Phys. B8, 1795 (1975); 9, 1221 (1976); R. Salomaa, ibid 10, 3005 (1977).
8. Additional references may be found in Laser Spectroscopy III edited by J.L. Hall and J.L. Carlsten (Springer-Verlag, New York, 1977); Nonlinear Laser Spectroscopy, V.S. Letokhov and V.P. Chebotaev (Springer-Verlag, New York, 1977); High Resolution Laser Spectroscopy edited by K. Shimoda (Springer-Verlag, New York, 1976); Laser Spectroscopy of Atoms and Molecules edited by H. Walther (Springer-Verlag, New York, 1976); Frontiers in Laser Spectroscopy edited by R. Balian, S. Haroche and S. Liberman (North-Holland, Amsterdam, 1977).
9. K. Shimoda in High Resolution Laser Spectroscopy (K. Shimoda, ed., Springer-Verlag, New York, 1976) p. 11.
10. S. Stenholm, J. Phys. B10, 761 (1977).

References - Con't,

11. P.R. Berman, in Advances in Atomic and Molecular Physics edited by D.R. Bates and B. Bederson (Academic Press Inc., New York, 1977) Vol. 13, p. 57.

12. P.R. Berman, Phys. Reports 43, 101 (1978).

13. A.P. Kolchenko, A.A. Pukhov, S.G. Rautian and A.M. Shalagin, Zh. Eksp. Teor. Fiz. 63, 1173 (1972) [Sov. Phys. - JETP 36, 619 (1973)].

14. V.P. Kochanov, S.G. Rautian and A.M. Shalagin, Zh. Eksp. Teor. Fiz. 72, 1358 (1977) [Sov. Phys. - JETP 45, 714 (1977)].

15. L. Klein, M. Giraud, and A. Ben-Reuven, Phys. Rev. A16, 289 (1977).

16. Extensive additional references may be found in Ref. 11 and in a review article by Berman [P.R. Berman. Appl. Phys. (Germany) 6, 283 (1975)].

17. P.R. Liao, J.E. Bjorkholm and P.R. Berman,

18. P.R. Berman, Phys. Rev. A5, 927 (1972).

19. J.L. LeGouët, uppublished.

20. S.G. Rautian and A.A. Feoktistov, Zh. Eksp. Teor. Fiz. 56, 227 (1969) [Sov. Phys. - JETP 29, 126 (1969)].

21. S.R. Drayson, J, Quant. Spectroc. Radiat. Transfer 16, 611 (1976).

22. J. Keilson and K.E. Storer, Q. Appl. Math. 10, 243 (1952).

23. Equation 59b is a somewhat better asymptotic form than that given in Ref. 11.

24. P.R. Berman, Phys. Rev. A13, 2191 (1976).

References - Con't.

25. To avoid indeterminate factors in the saturation parameter at zero pressure, we actually take $\gamma_1 = 0.0001$ and $\gamma_2 = \gamma_2' + .0001$. These small additions to γ_1 and γ_2 may be thought to simulate transit-time effects.

Figure Captions

Fig. 1. The three-level systems considered in this work: (a) upward cascade, (b) inverted V, (c) V. Note that the total decay rate from level 2 is γ_2.

Fig. 2. Line shape $I_s(\Delta,\Delta')/\chi^2$ in arbitrary units for the case $N_{32} = 0$, $\Delta = -1$, $P = 0$, $\epsilon = 1$ (broken line) or $\epsilon = -1$ (solid line) and several χ. All frequencies are in units of ku and P is in Torr. For values of other parameters, see the text. Note that, in all displayed line shapes, $\beta = \beta' = 1$ (upward cascade).

Fig. 3. Line shape for $N_{21} = 0$, $\Delta = -1$, $P = 0$, $\epsilon = -1$ and several χ. Units are as in Fig. 2. The same arbitrary units for I_s/χ^2 are used in all the figures.

Fig. 4. Line shape for $N_{32} = 0$, $\Delta = -10$, $\epsilon = -1$, $\chi = 0.01$ and several P. The resonances centered about $\Delta' = 10$ vary only slightly in the pressure range studied.

Fig. 5. Line shape for $N_{21} = 0$, $\Delta = -10$, $\epsilon = -1$, $\chi = 0.01$ and several P. The line shape changes only slightly in the pressure range $P = 0$ to 2.

Fig. 6. Line shape for $N_{32} = 0$, $\Delta = -1$, $\epsilon = -1$, $\chi = 1.0\times10^{-4}$, and several pressures, P.

Fig. 7. Line shape for $N_{32} = 0$, $\Delta = -1$, $\epsilon = -1$, $\chi = 0.2$ and several pressures, P.

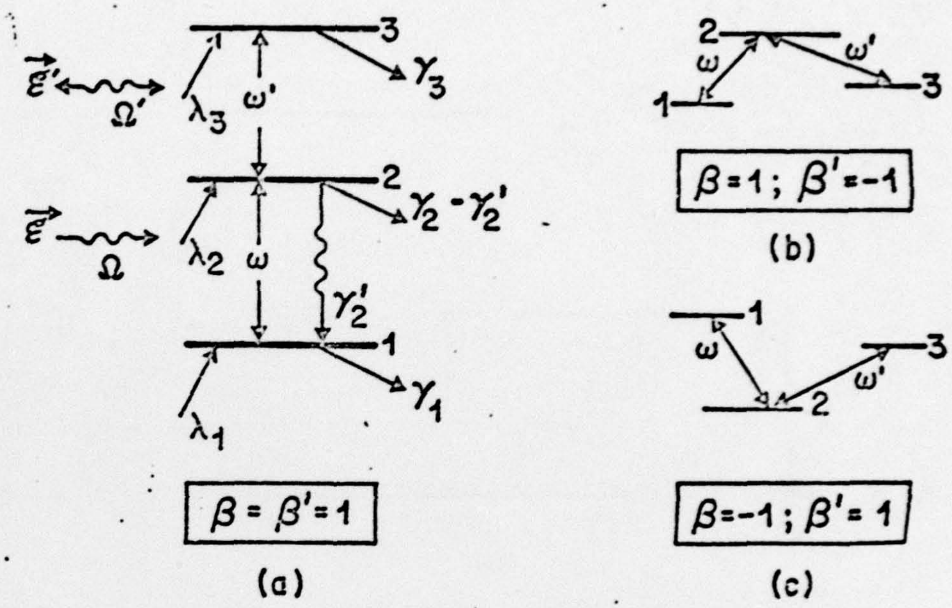

Fig. 1

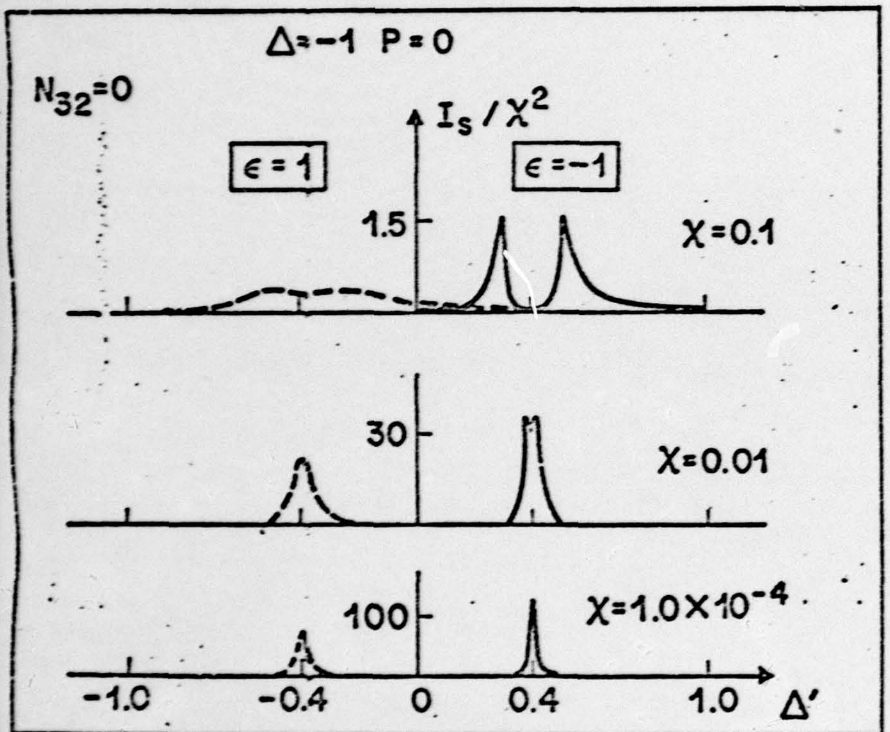

Δ=-1 P=0
N32=0
Is/X2
ε=1
ε=-1
1.5
X=0.1
30
X=0.01
100
X=1.0X10-4
-1.0
-0.4
0
0.4
1.0
Δ'

Fig. 2

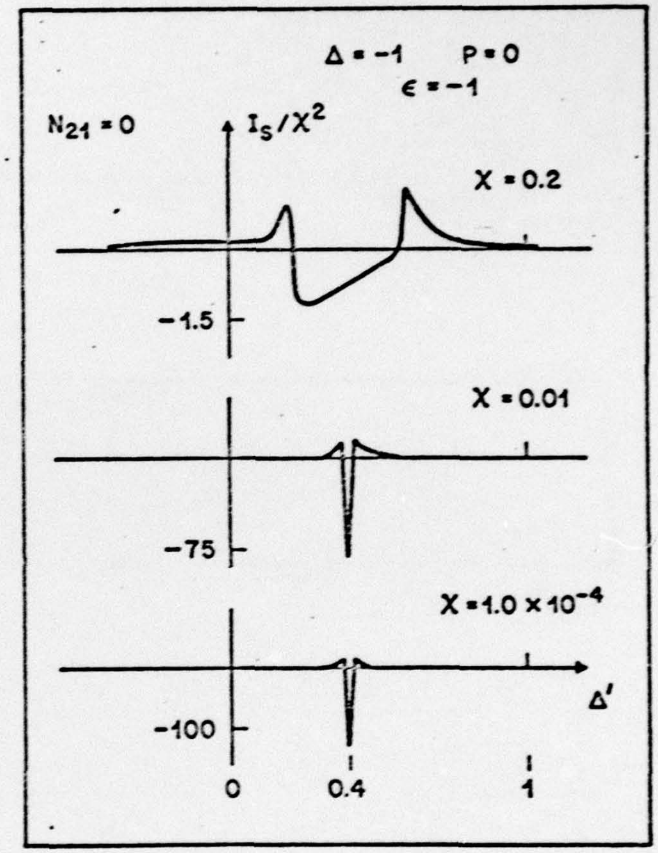

Δ=-1 P=0
ε=-1
N21=0
Is/X2
X=0.2
-1.5
X=0.01
-75
X=1.0×10-4
Δ'
-100
0
0.4
1

Fig. 3

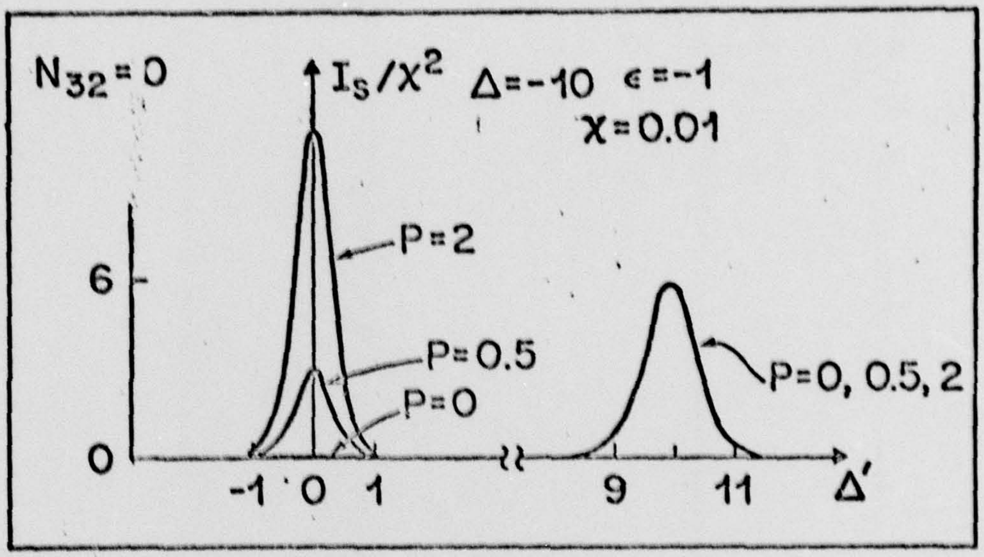
$N_{32}=0$
I_S/X^2
$\Delta=-10$ $\epsilon=-1$
$X=0.01$
P=2
6
P=0.5
P=0
P=0, 0.5, 2
0
-1
0
1
9
11
Δ'

Fig. 4

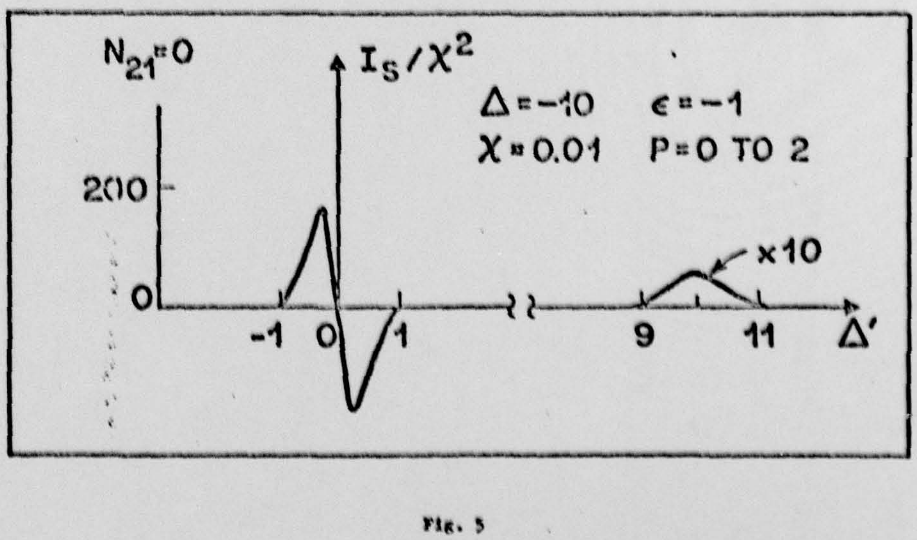
$N_{21}=0$
I_S/X^2
$\Delta=-10$ $\epsilon=-1$
$X=0.01$ P=0 TO 2
200
x10
0
-1
0
1
9
11
Δ'

Fig. 5

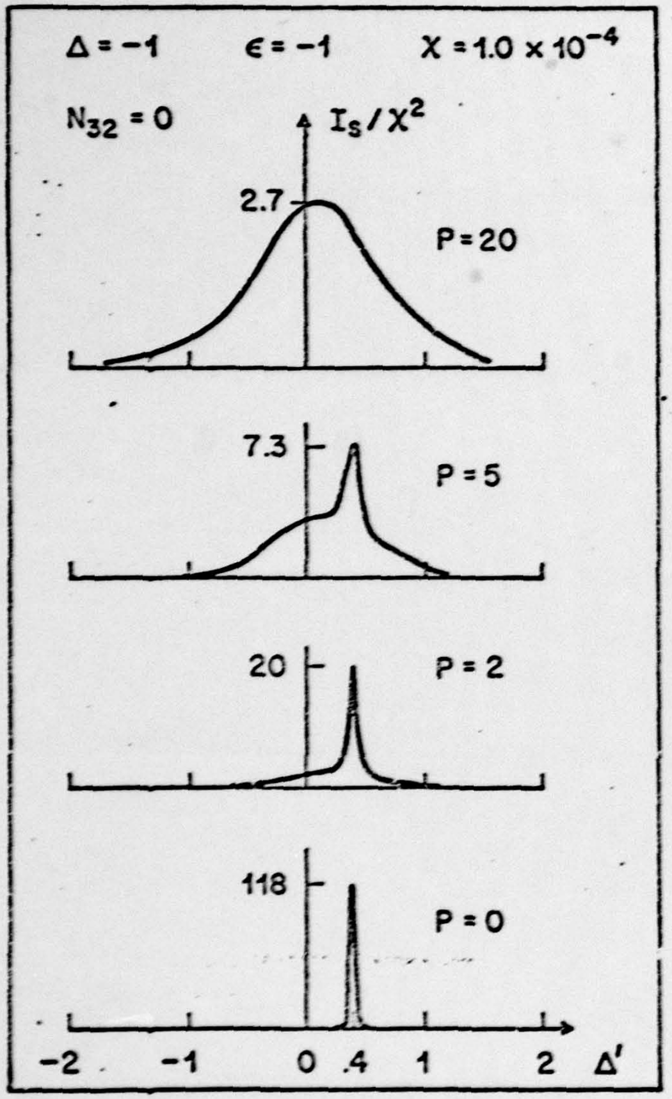

Δ = −1
ϵ = −1
χ = 1.0 × 10⁻⁴
N₃₂ = 0
Iₛ/χ²
2.7
P = 20
7.3
P = 5
20
P = 2
118
P = 0
−2
−1
0
.4
1
2
Δ′

Fig. 6

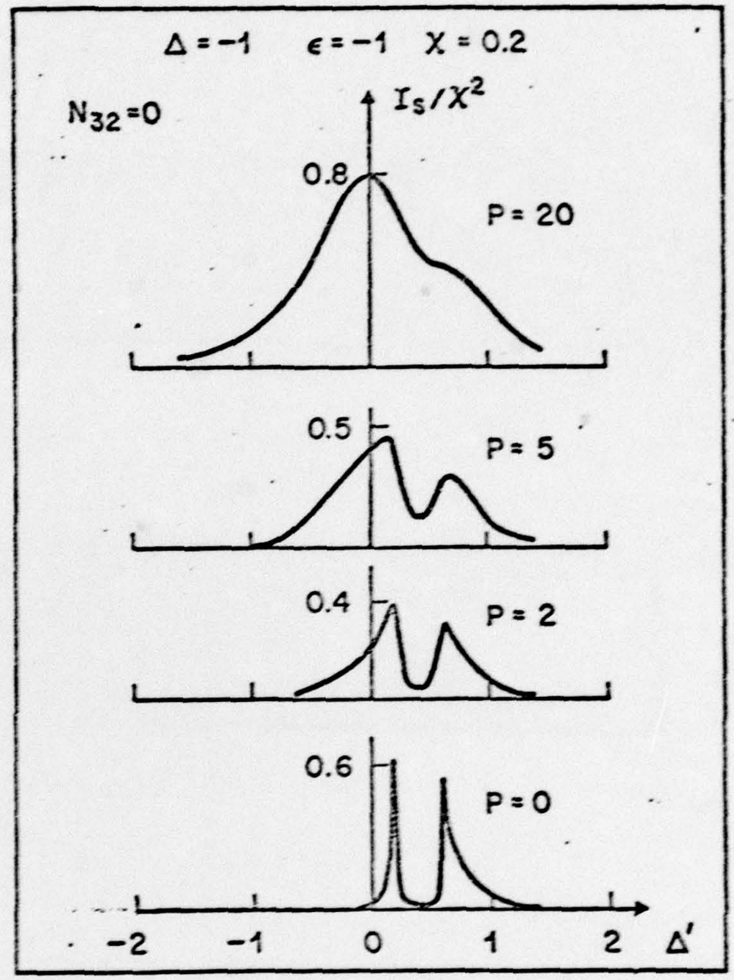

Δ = −1
ϵ = −1
χ = 0.2
N₃₂ = 0
Iₛ/χ²
0.8
P = 20
0.5
P = 5
0.4
P = 2
0.6
P = 0
−2
−1
0
1
2
Δ′

Fig. 7